

Phosphinite-Iminopyridine Iron Catalysts for Chemoselective Alkene Hydrosilylation

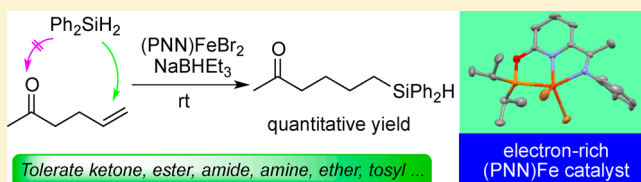
Dongjie Peng,[†] Yanlu Zhang,[†] Xiaoyong Du,[†] Lei Zhang,[†] Xuebing Leng,[†] Marc D. Walter,^{*,‡} and Zheng Huang^{*,†}

[†]State Key Laboratory of Organometallic Chemistry, Shanghai Institute of Organic Chemistry, Chinese Academy of Science, 345 Lingling Road, Shanghai 200032, P.R. China

[‡]Institut für Anorganische und Analytische Chemie, Technische Universität Braunschweig, Hagenring 30, 38106 Braunschweig, Germany

Supporting Information

ABSTRACT: A series of new pincer iron complexes with electron-donating phosphinite-iminopyridine (PNN) ligands has been prepared and characterized. These iron compounds are efficient and selective catalysts for the anti-Markovnikov alkene hydrosilylation of primary, secondary, and tertiary silanes. More importantly, the system exhibits unprecedented functional group tolerance with reactive groups such as ketones, esters, and amides. Furthermore, the iron-catalyzed alkene hydrosilylation was successfully applied to the synthesis of a valuable insecticide, silafluofen. The electronic properties and structures of the iron complexes have been studied by spectroscopies and computational methods. Overall, the iron catalysts may provide a low-cost and environmentally benign alternative to currently employed precious metal systems for alkene hydrosilylation.



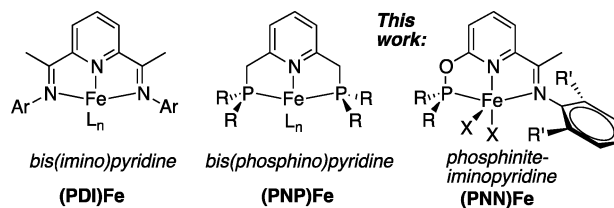
1. INTRODUCTION

Alkene hydrosilylation is one of the largest volume reactions conducted with homogeneous catalysts in chemical industry.¹ Alkylsilanes produced from alkene hydrosilylations are widely used as raw materials in manufacturing silicon rubbers, molding implants, releasing coatings, and adhesives.² To date, alkene hydrosilylation has been dominated by the use of Pt catalysts such as Speier's and Karstedt's complexes.³ However, platinum is an extremely rare metal. The low abundance, high cost, and environmental issues concerning heavy metals has motivated the investigation of safer and inexpensive alternatives.⁴ In this respect, catalysts based on earth-abundant and environmentally benign Fe are highly attractive for alkene hydrosilylation.

In fact, iron carbonyl complexes-catalyzed alkene hydrosilylations have been known for half a century; however, these systems often require photolysis to generate the active catalyst,⁵ and undesired side reactions, such as dehydrogenative silylation, compete with alkene hydrosilylation.^{5a,6} A key breakthrough was the report by the Chirik group of iron complexes with redox-active bis(imino)pyridine (PDI) ligands (Chart 1). The (PDI)Fe systems are remarkably efficient for selective anti-Markovnikov alkene hydrosilylation with various silanes and it is also compatible with functionalized alkenes including *N,N*-dimethylallylamine and allyl polyethers,^{7,8} and the redox-activity of the noninnocent bis(imino)pyridine ligands was believed to play an essential role in the catalysis.^{8b,9}

Broad functional group compatibility is of paramount importance for the general synthetic applications of alkene hydrosilylation in organic synthesis. Despite significant improvements in terms of catalytic efficiency employing Fe

Chart 1. PDI, PNP, and PNN Iron Complexes

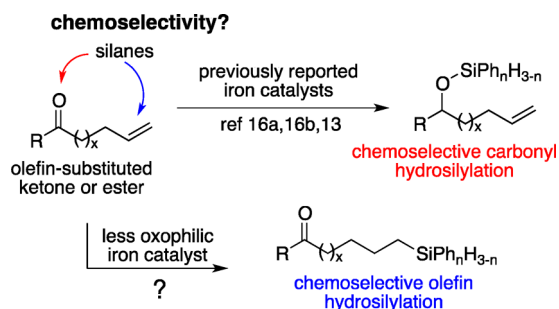


complexes with bis(imino)pyridine ligands, the functionalized alkene substrates have been limited to amino-, polyether-, and epoxide-substituted olefins.^{7b,8b} In comparison, Pt and Rh catalysts have also been used for hydrosilylation of alkenes with amides, ketones, esters and amines functionalities.^{3g,10} These transformations incorporate silicon to highly functionalized systems, allowing facile synthesis of biologically active silicon-containing peptides^{10a} and insecticides,¹¹ as well as surface-functionalized luminescent silicon nanoparticles.¹² In contrast, iron-catalyzed chemoselective hydrosilylation of alkenes containing carbonyl group has remained unknown. Since the first row transition metals are in general more oxophilic than the second and third row late transition metals, iron-catalyzed ester,¹³ amide,¹⁴ or ketone¹⁵ hydrosilylation can compete favorably with alkene hydrosilylation. Indeed, in the reactions of olefin-substituted carbonyl compounds, all previously reported iron catalysts effected chemoselective ketone¹⁶ and

Received: May 17, 2013

ester¹³ hydrosilylation, but no alkene hydrosilylation (Scheme 1).¹⁷

Scheme 1. Chemoselectivity in Hydrosilylation of Olefin-Substituted Ketone and Ester



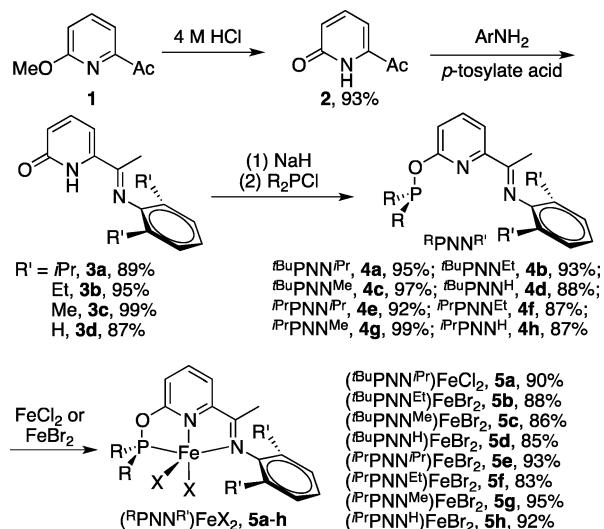
To fully replace the Pt, Rh, and other precious metals with Fe in catalytic alkene hydrosilylation, the functional group compatibility of the latter must be improved. We envisioned that the utilization of electron-donating pincer phosphine ligands might result in an electron-rich Fe center, and thus reduce the oxophilicity on the metal and potentially improve its tolerance toward functional groups. In fact, bis-(dialkylphosphino)pyridine¹⁸ (Chart 1), a redox-inactive PNP-type ligand, has proven to be more electron-donating than the bis(imino)pyridine ligands.^{18a} Unfortunately, the PNP iron complex exhibited no activity in alkene hydrosilylation because of facile catalyst decomposition via ligand dissociation.^{18a}

Guided by these precedents, we sought to develop less oxophilic iron complexes with improved stability using electron-donating PNN-type ligands. A couple of PNN pincer iron complexes have been reported,^{18b} and very recently, we have shown that an iron complex bearing Milstein's electron-donating bipyridyl-based phosphine pincer ligand catalyzes alkene hydroboration.¹⁹ Herein, we report on a series of new (PNN)Fe complexes using novel phosphinite-iminopyridine ligands (Chart 1). These complexes are efficient catalyst precursors for anti-Markovnikov alkene hydrosilylation with primary, secondary, and tertiary silanes. More importantly, the iron catalysts tolerate a wide range of organic functional groups, and for the first time, iron-catalyzed chemoselective hydrosilylation of alkenes containing amide, ester, and ketone functionalities has been achieved.

2. RESULTS AND DISCUSSION

2.1. Preparation of the PNN Ligands and Iron Dihalide Complexes. The synthesis of the $^R\text{PNN}^R$ ligands and the corresponding iron complexes is outlined in Scheme 2. Deprotection of the methoxy group of 2-acetyl-6-methoxypyridine **1** with HCl formed 6-acetyl-2(1H)-pyridinone **2**, which undergoes Schiff-base condensation with arylamines bearing various substituents at the 2,6-aryl positions to give the respective imines **3a–d** in high yields. Deprotonation with NaH, followed by the addition of dialkylchlorophosphine, generated the PNN phosphinite-iminopyridines ligands **4a–h** in 87–99% yield. The neutral Fe(II) dihalide complexes ($^R\text{PNN}^R$)FeX₂ (R = *t*Bu, R' = *i*Pr, **5a**; R = *t*Bu, R' = Et, **5b**; R = *t*Bu, R' = Me, **5c**; R = *t*Bu, R' = H, **5d**; R = *i*Pr, R' = *i*Pr, **5e**; R = *i*Pr, R' = Et, **5f**; R = *i*Pr, R' = Me, **5g**; R = *i*Pr, R' = H, **5h**) were prepared by the addition of ligands to the anhydrous iron

Scheme 2. Synthesis of ($^R\text{PNN}^R$)FeX₂ Complexes **5a–h**



salts. These iron complexes are paramagnetic, high-spin Fe^{II} species, as indicated by magnetic susceptibility measurements (see Experimental Section for details). Their ¹H NMR resonances are broadened and paramagnetically shifted.

Complexes ($^t\text{BuPNN}^i\text{Pr}$)FeCl₂ (**5a**) with the most bulky ligand and ($^i\text{PrPNN}^{\text{H}}$)FeBr₂ (**5h**) with the least bulky ligand were also characterized by X-ray diffraction analyses. The solid structures of **5a** and **5h** reveal a distorted square-pyramidal geometry at the mononuclear iron site (Figure 1). Regardless of the ortho-aryl and phosphino substituents, the planes of the

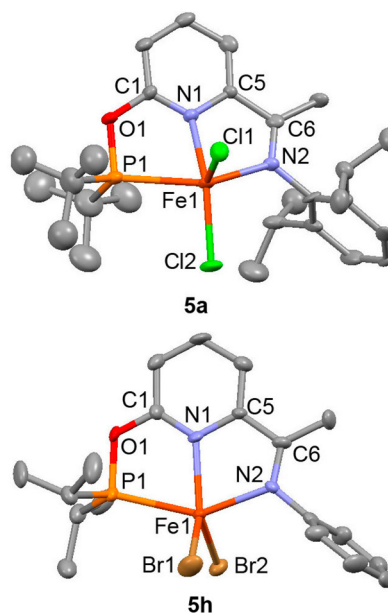


Figure 1. ORTEP diagrams of complexes **5a** and **5h**. Thermal ellipsoids shown at 50% probability. Selected bond distances (Å) and angles (deg) for **5a**: Fe1–N1, 2.203(6); Fe1–N2, 2.185(6); Fe1–P1, 2.571(2); Fe1–Cl1, 2.297(2); Fe1–Cl2, 2.316(2); C6–N2, 1.292(9); C5–C6, 1.490(10); N1–Fe1–N2, 73.2(2); N1–Fe1–P1, 72.55(16); P1–Fe1–N2, 138.46(16); Cl1–Fe1–Cl2, 113.57(9). For **5h**: Fe1–N1, 2.187(7); Fe1–N2, 2.178(8); Fe1–P1, 2.528(3); Fe1–Br1, 2.4383(18); Fe1–Br2, 2.4634(17); C6–N2, 1.301(12); C5–C6, 1.471(13); N1–Fe1–N2, 274.0(3); N1–Fe1–P1, 73.4(2); P1–Fe1–N2, 147.0(2); Br1–Fe1–Br2, 106.37(6).

aryl rings are essentially orthogonal to the plane defined by the two nitrogen and one phosphorus atoms.

2.2. (PNN)Fe-Catalyzed Hydrosilylation of 1-Octene with Primary, Secondary, and Tertiary Silanes. Complexes **5a–h** were tested as precatalysts for the hydrosilylation of a nonpolar olefin with primary, secondary, and tertiary silanes, respectively. Our studies commenced with the reaction of 1-octene with the primary silane PhSiH₃, and these results are summarized in Table 1. The active catalysts were generated

Table 1. (PNN)Fe Precatalysts **5a–h for Alkene Hydrosilylation with Primary, Secondary, and Tertiary Silanes^a**

$\text{C}_6\text{H}_{13}\text{CH=CH}_2 + \text{R}_n\text{SiH}_{4-n} \xrightarrow[\text{23 } ^\circ\text{C, 3 h}]{\text{2x mol \% NaBHET}_3, \text{toluene}} \text{C}_6\text{H}_{13}\text{CH}_2\text{CH}_2\text{SiR}_n\text{H}_{3-n}$					
0.6 mmol		0.6 mmol		$\text{R}_n\text{H}_{3-n} = \text{PhH}_2 \text{ (8)}, \text{Ph}_2\text{H} \text{ (9)},$ $(\text{EtO})_3 \text{ (10)}, (\text{Me}_3\text{SiO})_2\text{Me} \text{ (11)}$	
precatal.	silane	% yield	precatal.	silane	% yield
5a	PhSiH ₃	94	5e	PhSiH ₃	91
	Ph ₂ SiH ₂	—:38:12 ^b		Ph ₂ SiH ₂	99
	(EtO) ₃ SiH	NR		(EtO) ₃ SiH	NR
	MD'M	NR		MD'M	NR
5b	PhSiH ₃	89	5f	PhSiH ₃	38 ^b
	Ph ₂ SiH ₂	53:6:4 ^b		Ph ₂ SiH ₂	75:7:— ^b
	(EtO) ₃ SiH	52:10:— ^b		(EtO) ₃ SiH	95
	MD'M	NR		MD'M	91
5c	PhSiH ₃	99	5g	PhSiH ₃	24 ^b
	Ph ₂ SiH ₂	50:20:5 ^b		Ph ₂ SiH ₂	98
	(EtO) ₃ SiH	42:13:— ^b		(EtO) ₃ SiH	91
	MD'M	NR		MD'M	72
5d	PhSiH ₃	15:12:2 ^b	5h	PhSiH ₃	0
	Ph ₂ SiH ₂	55:18:3 ^b		Ph ₂ SiH ₂	99
	(EtO) ₃ SiH	85		(EtO) ₃ SiH	90
	MD'M	NR		MD'M	82

^aFor PhSiH₃: 1 mol % Fe precatalyst and 2 mol % NaBHET₃; For Ph₂SiH₂ and (EtO)₃SiH: 2 mol % Fe precatalyst and 4 mol % NaBHET₃; For MD'M: 5 mol % Fe precatalyst and 10 mol % NaBHET₃. Reported yields are isolated yields (average of three runs) unless otherwise noted. ^bRatio of hydrosilylation product: allylsilane: (*E*)-vinylsilane. Yields were determined by ¹H NMR with an internal standard.

in situ upon the addition of NaBHET₃ (2 equiv) to the precursors **5a–h**.²⁰ Using the relatively bulky complexes (^tBuPNNⁱPr)⁺FeCl₂[−] (**5a**), (^tBuPNN^{Et})⁺FeBr₂[−] (**5b**), (^tBuPNN^{Me})⁺FeBr₂[−] (**5c**), and (ⁱPrPNNⁱPr)⁺FeBr₂[−] (**5e**), the reactions proceeded efficiently at 23 °C to give the anti-Markovnikov product **6** in 89–99% isolated yields after 3 h.²¹ In contrast, the reactions with less sterically hindered complexes gave low yields of **6** due to competing side reactions. With **5d** as the precatalyst, dehydrogenative hydrosilylation occurred to give 12% allylsilane and 2% (*E*)-vinylsilane. Using **5f–h** as the precatalysts, varying amounts of Ph₂SiH₂ were formed from the redistribution of PhSiH₃ (see Supporting Information (SI) for product distributions). In an extreme case, the reaction with the least hindered precatalyst **5h**, no hydrosilylation product was detected; instead, Ph₂SiH₂ (12%) was formed.

Iron-catalyzed alkene hydrosilylation with secondary silane, Ph₂SiH₂, is typically slower than the corresponding reaction with PhSiH₃ and often proceeds with only poor conversion.^{7a,8a} Whereas complex (^tBuPNNⁱPr)⁺FeCl₂[−] **5a** is highly efficient for the hydrosilylation of 1-octene with Ph₃SiH, no hydrosilylation

product was obtained from the reaction of 1-octene with Ph₂SiH₂ using precatalyst **5a**; instead dehydrogenative hydrosilylation occurred to form allylsilane (38%) and (*E*)-vinylsilane (12%) (Table 1). In contrast, reducing the steric demand of the 2,6-aryl substituents has an advantageous effect on the hydrosilylation with Ph₂SiH₂. Reactions with complexes **5b,c** afforded the desired product **7** after 3 h in ~50% yields, but moderate amounts of products attributed to dehydrogenative hydrosilylation were also detected (Table 1). Notably, *i*Pr-for-*t*Bu substitution on the P atom of the PNN ligands apparently has a more favorable effect than the variation of the ortho-aryl substituents. While hydrosilylation with (ⁱPrPNN^{Et})⁺FeBr₂[−] (**5f**) gave 75% of **7** and 7% of allylsilane, reactions with precatalysts **5e**, **5g**, and **5h** exclusively formed the hydrosilylation product **7** in nearly quantitative yields (98–99%).

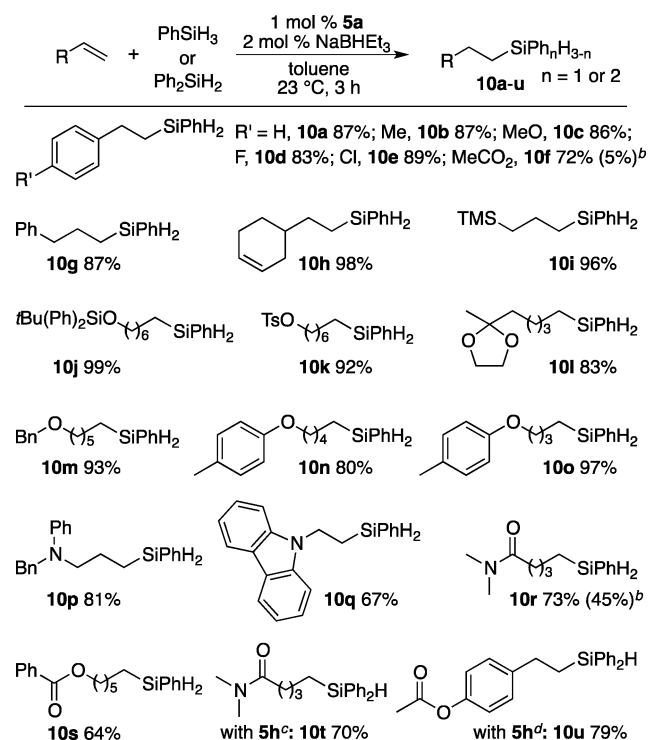
Generally tertiary silanes are less reactive than primary and secondary silanes for alkene hydrosilylation.^{7b,8b} As expected, no alkene hydrosilylation was observed with (EtO)₃SiH and the most sterically demanding complexes **5a** and **5e**. Nevertheless **5b** and **5c** exhibited moderate activity for the addition of (EtO)₃SiH, but dehydrogenative hydrosilylation also occurred to give allylsilane as a side product. Gratifyingly, complexes with reduced steric crowding (**5d**, and **5f–h**) are efficient for the hydrosilylation with (EtO)₃SiH, giving the anti-Markovnikov product **8** exclusively in excellent isolated yields (85–95%, Table 1).²²

In addition, hydrosilylation of 1-octene with the industrially important (Me₃SiO)₂MeSiH (MD'M) using precatalysts **5f** (87%), **5g** (72%), and **5h** (82%) proceeded smoothly at ambient temperature to give the desired product **9** in high yields (Table 1). Complexes **5a–e** exhibit no activity for the hydrosilylation with MD'M.

2.3. (PNN)Fe-Catalyzed Hydrosilylation of Functionalized Alkenes. A large number of functionalized alkenes underwent hydrosilylation with silanes in high yield at ambient temperature using the PNN iron system. These results are summarized in Scheme 3. Using complex **5a** as the precatalyst, styrene and its derivatives bearing electron-donating or electron-withdrawing substituents were efficiently hydrosilylated with PhSiH₃ to form the linear products **10a–f** in 72–89% isolated yields. γ -Phenylpropene was also hydrosilylated in high yield (**10g**, 87%). Furthermore, the hydrosilylation of 4-vinyl-cyclohexene occurred selectively at the terminal olefin to give **10h** in 98% isolated yield. The reaction of allyltrimethylsilane afforded the product **10i** in 96% yield. Aliphatic alkenes containing protecting groups, such as a silyl ether (TBDDS, **10j**, 99%) and a tosylate (**10k**, 92%), also underwent hydrosilylation in high yields. In addition, ketals are also tolerated as demonstrated by the isolation of **10l** in 83% yield.

Ether functionalities including an allyl ether moiety are tolerated as shown by isolation of hydrosilylation products **10m–o** in 80–97% yields. Furthermore, these iron catalysts are also compatible with amino-substituted alkenes. Hydrosilylation of *N*-allyl-*N*-phenylbenzylamine and 9-vinyl-carbazole formed the desired products **10p** and **10q** in 81 and 67% isolated yields, respectively.

Overall, the PNN iron system significantly enhances the synthetic utility of hydrosilylation by catalyzing addition of silanes to alkenes containing carbonyl groups. Reaction of amide- and ester-substituted olefins with PhSiH₃ underwent chemoselective alkene hydrosilylation with 1 mol % iron complex **5a** to form products **10f**, **10r**, and **10s** in 72, 73, and 64% isolated yields, respectively. For comparison, the same

Scheme 3. (PNN)Fe-Catalyzed Hydrosilylation of Functionalized Alkenes^a

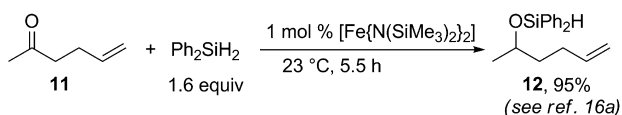
^aReported yields are isolated yields. ^bThe values in parentheses are ¹H NMR yields for the reactions using 1 mol % (ⁱPrPDI)Fe(N₂)₂ as the catalyst; ^c2 mol % 5a and 4 mol % NaBHET₃; ^d4 mol % 5a and 8 mol % NaBHET₃.

reactions using the related bis(imido)pyridine iron complex (ⁱPrPDI)Fe(N₂)₂ as the catalyst gave the products **10f** (5%) and **10r** (45%) in much lower yields (see Scheme 3). Reaction of these olefins with the secondary silane Ph₂SiH₂ using **5h** also occurred to give, after 3 h, **10t** (70%) and **10u** (79%) in synthetically useful yields.

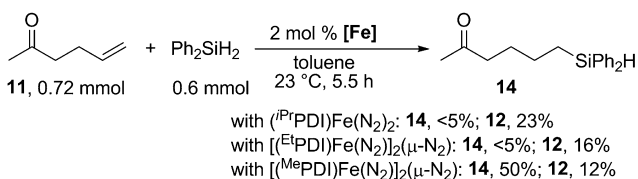
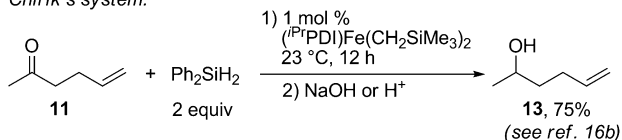
2.4. (PNN)Fe-Catalyzed Hydrosilylation of Ketone-Functionalized Alkenes. Next, we investigated iron-catalyzed hydrosilylation of alkenes bearing ketone functionalities. In general, ketones are highly reactive groups and can readily undergo hydrosilylation in the presence of various iron catalysts.^{15,16} Thus, selective alkene hydrosilylation in the presence of ketone functionalities is very challenging. Indeed, Tilley et al. reported that the iron amide catalyst [Fe{N(SiMe₃)₂}]₂ is selective for ketone hydrosilylation of 5-hexen-2-one (**11**) with Ph₂SiH₂ to give the silyl ether **12** in 95% yield (Scheme 4).^{16a} Using the bis(imino)pyridine Fe catalyst (ⁱPrPDI)Fe(CH₂SiMe₃)₂, Chirik et al. have shown that **11** underwent selective ketone reduction with Ph₂SiH₂ to form 5-hydroxy-1-hexene (**13**) in 75% yield with no evidence for alkene reduction (Scheme 4).^{16b} Since bis(imino)pyridine Fe complexes with smaller aryl substituents might be superior to (ⁱPrPDI)Fe(N₂)₂ in alkene hydrosilylations,^{7b} we also carried out the hydrosilylation of **11** with Ph₂SiH₂ using Chirik's iron dinitrogen complexes with varying steric demand. Consistent with Chirik's report, (ⁱPrPDI)Fe(N₂)₂ is inactive for alkene hydrosilylation of **11**. Whereas the reaction with [(^{Et}PDI)Fe(N₂)₂](μ-N₂) also gave negligible amounts of the alkene hydrosilylation product **14**, the less sterically encumbered derivative [(^{Me}PDI)Fe(N₂)₂](μ-N₂) gave 50% of **14** (¹H NMR

Scheme 4. Opposite Chemoselectivity in Hydrosilylation of 5-Hexen-2-one with Ph₂SiH₂ Catalyzed by Tilley's, Chirik's, and PNN Iron Complexes

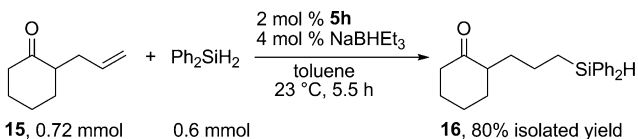
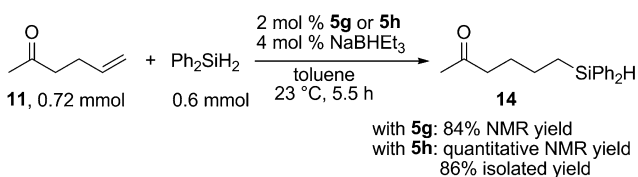
Tilley's system:



Chirik's system:



(PNN)Fe system, this work:

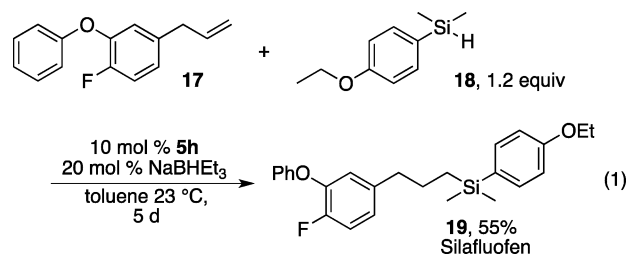


yield) (Scheme 4). Varying amounts of the ketone hydrosilylation product **12** were observed in the reactions with the three (PDI)Fe dinitrogen catalysts (Scheme 4).

Given the high efficiency of **5g** and **5h** in the hydrosilylation of 1-octene with Ph₂SiH₂ (vide supra) we used these complexes as precatalysts for the hydrosilylation of 5-hexen-2-one (**11**). It is noteworthy that the reaction of **11** with Ph₂SiH₂ using **5g** at 23 °C afforded 84% of the alkene hydrosilylation product **14** (¹H NMR yield) after 5.5 h. When complex **5h** was employed, **11** underwent exclusively alkene hydrosilylation in quantitative yield as determined by ¹H NMR spectroscopy (86% isolated yield) (Scheme 4). In both reactions, no carbonyl reduction product **12** was detected. Similarly, the reaction of 2-allylcyclohexanone **15** with Ph₂SiH₂ catalyzed by **5h** exclusively formed the desired product **16** in 80% isolated yield (Scheme 4).

2.5. Synthesis of the Insecticide Silafluofen by Iron-Catalyzed Alkene Hydrosilylation. To demonstrate the synthetic value of the PNN iron-catalyzed alkene hydrosilylation, **5h** was applied to the synthesis of the novel pyrethroid-like insecticide, silafluofen. Silafluofen is an attractive agricultural insecticide because of its high insecticidal activity, low toxicity, and good stability. The key step in the industrial preparation of silafluofen requires the expensive Speier's platinum catalyst for alkene hydrosilylation under rather harsh reaction condition (130 °C).¹¹ To our delight, with **5h** (10 mol %) as the precatalyst, the reaction of 3-(4-

fluoro-3-phenoxyphenyl)-1-propene (**17**) and (4-methoxyphenyl)dimethylsilane (**18**) occurred at 23 °C to form the desired product silafluofen (**19**) in 55% isolated yield (eq 1).



2.6. Unreactive Substrates in (PNN)Fe-Catalyzed Hydrosilylation. A list of unreactive olefin substrates is provided in Figure 2. Internal olefins, such as 2-hexene and

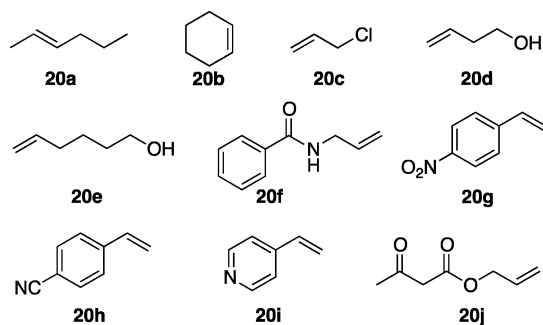
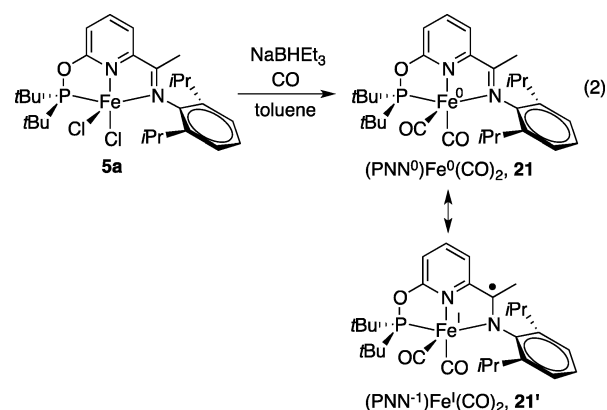


Figure 2. Unreactive hydrosilylation substrates.

cyclohexene, are unreactive for (PNN)Fe-catalyzed hydrosilylation with PhSiH_3 or Ph_2SiH_2 . Reactions of allyl chloride (**20c**) and alkenes bearing unprotected alcohols (**20d** and **20e**) and amide with an NH group (**20f**) also yielded no hydrosilylation product. Furthermore, no reaction of styrene derivatives containing nitro (**20g**), nitrile (**20h**), or pyridine (**20i**) units was observed, and allyl acetoacetate (**20j**) likely poisons the catalyst by metal chelation.

2.7. Electronic Properties and Electronic Structure of the PNN Iron Fragment. The results described above clearly show that the (PNN)Fe catalysts are tolerant of a variety of functional groups and chemoselective for alkene hydrosilylations in the presence of these functionalities. We presumed that the excellent functional group compatibility results from the less oxophilic nature of the (PNN)Fe complex. To confirm this hypothesis, it is of interest to study the electronic properties and electronic structure of the PNN iron fragment.

2.7.1. Electronic Properties of the PNN Iron Fragment Investigated by IR Spectroscopies and Electrochemical Measurements. A useful tool to evaluate the electron-donating ability of the phosphinite-iminopyridine ligands is the ν_{CO} stretching frequencies of the respective carbonyl complexes. Carbonyl complex $(^t\text{BuPNN}^{\text{iPr}})\text{Fe}(\text{CO})_2$ (**21**) was obtained in 51% yield by the reaction of CO with **5a** in the presence of 2 equiv of NaBHET_3 (eq 2). The ν_{CO} stretching frequencies of **21** in pentane solution (1902 and 1956 cm^{-1}) are red-shifted from those of the related iron bis(imino)pyridine complex $(^{\text{iPr}}\text{PDI})\text{Fe}(\text{CO})_2$ (**22**) (1914 and 1974 cm^{-1}).²³ The data are consistent with a more electron-rich $(^t\text{BuPNN}^{\text{iPr}})\text{Fe}$ fragment as compared to the $(^{\text{iPr}}\text{PDI})\text{Fe}$ fragment, resulting in increased backbonding to the CO ligands in **21**.



We also conducted electrochemical measurements of the free $^t\text{BuPNN}^{\text{iPr}}$ ligand **4a** and the iron carbonyl complex **21** to study the electronic properties of the (PNN)Fe fragment using the same conditions as reported for the PDI system (see SI). For comparison, the reduction potentials of the PNN system and

Table 2. Cyclic Voltammetry Data for Ligands and Iron Dicarboxyl Complexes

ligand and cmpd	redn (V vs Fc/Fc ⁺)	oxidn (V vs Fc/Fc ⁺)
$^t\text{BuPNN}^{\text{iPr}}$	−2.74	—
$^{\text{iPr}}\text{PDI}^a$	−2.62	—
$(^t\text{BuPNN}^{\text{iPr}})\text{Fe}(\text{CO})_2$	−2.54	−0.65
$(^{\text{iPr}}\text{PDI})\text{Fe}(\text{CO})_2^a$	−2.46	−0.49

^aReference 24.

the related $^{\text{iPr}}\text{PDI}$ system²⁴ are included in Table 2. The $^t\text{BuPNN}^{\text{iPr}}$ ligand **4a** exhibits a reduction wave at a more negative reduction potential than the $^{\text{iPr}}\text{PDI}$ ligand (120 mV difference), implying that the $^t\text{BuPNN}^{\text{iPr}}$ ligand is more electron-donating than the $^{\text{iPr}}\text{PDI}$ system. The carbonyl complex $(^t\text{BuPNN}^{\text{iPr}})\text{Fe}(\text{CO})_2$ (**21**) exhibits a reversible oxidation potential and an irreversible reduction potential. Although we currently cannot determine the electronic structure of the oxidized and reduced species, the cyclic voltammetry data show that complex **21** is more readily oxidized by 160 mV and less easily reduced by 80 mV than the $(^{\text{iPr}}\text{PDI})\text{Fe}(\text{CO})_2$ (**22**), highlighting the electron-richness of the $(^t\text{BuPNN}^{\text{iPr}})\text{Fe}$ fragment.

2.7.2. Electronic Structure of the $(^t\text{BuPNN}^{\text{iPr}})\text{Fe}(\text{CO})_2$ Complex Fragment Investigated by X-ray Analysis and VT NMR Studies. In contrast to **5a–h**, the dark-blue complex $(^t\text{BuPNN}^{\text{iPr}})\text{Fe}(\text{CO})_2$ **21** displays narrow, well-resolved NMR resonances, and the chemical shifts are within the expected region for a diamagnetic molecule. We also succeeded in growing crystals of **21** suitable for an X-ray diffraction experiment, and in the solid state **21** adopts a pseudosquare planar-pyramidal geometry (Figure 3). Interestingly, the $\text{C}_{\text{imine}}-\text{N}_{\text{imine}}$ bond distance in **21** (1.344(6) Å) is significantly longer than that in the dihalide complexes **5a** (1.292(9) Å) and **5h** (1.301(12) Å), which might suggest that the phosphinite-iminopyridine ligand is reduced to a radical anion in **21**. Consistent with this hypothesis, the $\text{C}_{\text{imine}}-\text{C}_{\text{pyridine}}$ bond distance in **21** (1.404(7) Å) is shorter than those in **5a** (1.490(10) Å) and **5h** (1.471(13) Å). On the basis of solution magnetic susceptibility studies (see Experimental Section) the ground state of **5** can unambiguously be assigned as a high-spin

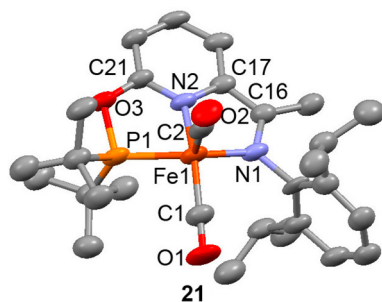


Figure 3. ORTEP diagram of complex **21**. Thermal ellipsoids shown at 50% probability. Selected bond distances (Å) and angles (deg): Fe1–N2, 1.913(4); Fe1–N1, 1.923(5); Fe1–P1 2.1768(18); Fe1–C1, 1.757(5); Fe1–C2, 1.787(7); C16–N1, 1.344(6); C16–C17, 1.404(7); C1–O1, 1.167(6); C2–O2, 1.156(7); N1–Fe1–N2, 79.18(18); N2–Fe1–P1, 79.80(15); P1–Fe1–N1, 148.40(14); C1–Fe1–C2, 95.7(3); N2–Fe1–C1, 158.9(2).

($S_{\text{Fe}} = 2$) ferrous center coordinated to the neutral PNN ligand. However, previous work by Lu and Wieghardt showed that α -iminopyridines are redox non-innocent ligands, and one notable structural feature of α -iminopyridyl radical anions is a significantly elongated $C_{\text{imine}}-N_{\text{imine}}$ bond and shortened $C_{\text{imine}}-C_{\text{pyridine}}$ bond distances consistent with an electron transfer into the LUMO of the α -iminopyridine ligand.²⁵ This raises the question regarding the electronic structure of **21**. Two pictures consistent with a singlet ground state ($S = 0$) may be developed, (a) a neutral PNN ligand is bound to a d^8 -Fe(0) $\text{Fe}(\text{CO})_2$ fragment with considerable π -backbonding into the LUMO of the α -iminopyridine system (closed-shell configuration, **21**), or alternatively (b) an open-shell case in which the $S_{\text{Fe}} = 1/2$ metal center and the PNN ligand radical anion ($S_{\text{PNN}} = 1/2$) (**21'**, see eq 2). Related arguments were developed with respect to the electronic ground state of $(^{\text{IPDI}}\text{Fe}(\text{CO})_2$ (**22**).²⁶

To gain insight in the electronic structure of **21** variable-temperature (VT) ^1H NMR studies have been undertaken, and the δ vs T^{-1} plots are shown in SI. No significant temperature dependence of the ^1H NMR chemical shifts was observed, consistent with a diamagnetic molecule. Furthermore, the temperature dependence of the ^1H NMR resonances is unchanged when the Me-group is exchanged with an H-atom in the α -iminopyridine moiety (see SI for details), arguing against the presence of unpaired spin density in these positions.²⁷

2.7.3. Electronic Structure of the (PNN)Fe Complexes
Fragment Investigated by DFT Calculations. To further elaborate this electronic structures of the (PNN)Fe complexes, DFT calculations were performed on **5a** and **21** at the B3LYP level of theory. In Figure 4, the experimental and calculated geometric parameters for both complexes **5a** and **21** are compared. For **5a** a reasonable agreement between experimental and calculated geometry was obtained (see Figure 4).

For complex **21**, the molecular structure of the closed-shell system was computed, and the calculated metric parameters are in good agreement with the experimental ones (Figure 4). The corresponding molecular orbital diagram obtained for **21** is presented in Figure 5. These representations display significant backbonding from the filled Fe d-orbitals to the π^* orbitals of the two CO ligands (HOMO–1, HOMO–2, and HOMO–3). In addition, the HOMO is composed of the $\text{Fe}_{d_{z^2}}$ orbital and the LUMO of the PNN ligand, which can be explained by a

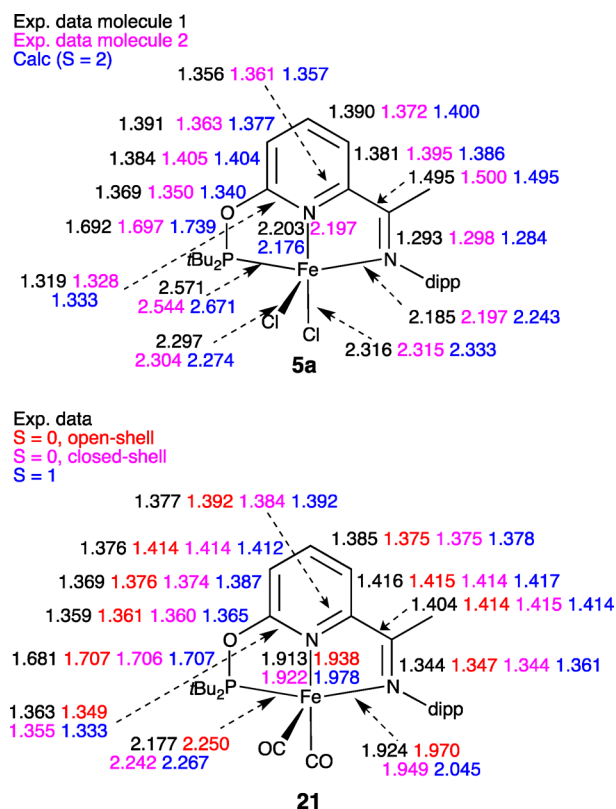


Figure 4. Comparisons between the X-ray structural data and calculated geometric parameters for both complexes **5a** and **21**. Note: the crystal structure of **5a** contains two molecules in the asymmetric unit.

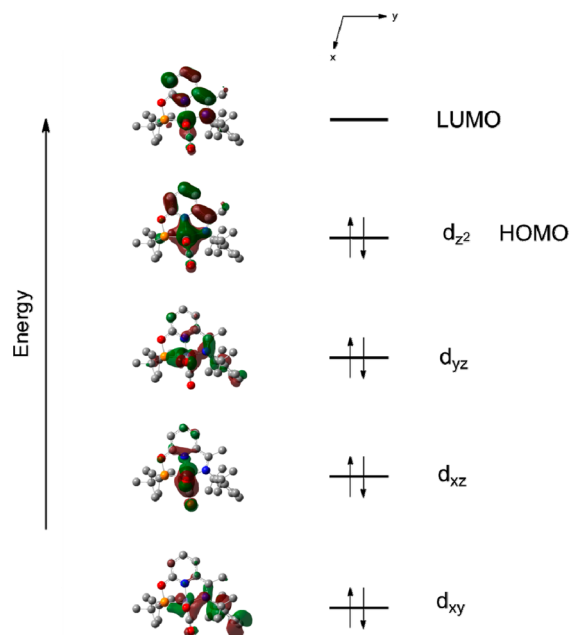


Figure 5. The molecular orbital diagram of complex **21** with a closed-shell singlet state spin configuration.

strong π -backbonding that gives rise to the observed contraction of the $C_{\text{imine}}-C_{\text{pyridine}}$ bond distance.

The geometry of the triplet state for **21** was also computed, and the most notable deviation between the calculated and

experimental structure was found for the Fe–N_{pyridine}, Fe–N_{imine}, and Fe–P bonds (Figure 4). Interestingly, enforcing an open-shell singlet state starting from the triplet state led to a geometry that is very similar to that of the closed-shell isomer (Figure 4).

The energy for the spin-unrestricted (open-shell singlet) calculation is slightly lower in energy than the closed-shell one (Figure 6). However, the electronic structure of complex **21** is

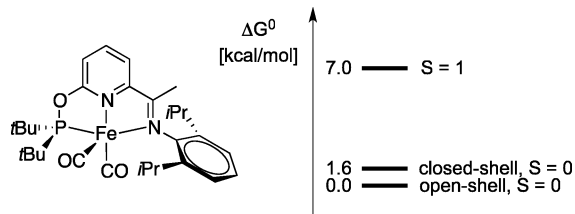


Figure 6. Energy differences between the triplet state, the closed-shell singlet state, and the open-shell singlet state for complex **21**.

probably best described as a delocalized (covalent) system with a charge distribution such as Fe(+I)–(PNN)^{1–}, but without significant diradical character consistent with the VT-NMR data (vide supra).²⁸ Further electronic structure studies are in progress and will be reported in due course.

2.8. Probing the Binding Affinities of Olefin Vs Carbonyl Functionalities toward the (PNN)Fe- and (PDI)Fe-Fragment. As demonstrated experimentally the (PNN)Fe systems exhibit unprecedented high chemoselectivity for hydrosilylation of alkenes bearing reactive functionalities, such as carbonyl groups. This selectivity has a steric component (as shown in section 2.4), but the electrochemical data also suggest electronic reasons, e.g. the (PNN)Fe complexes are more electron-rich than the related (PDI)Fe complexes. The elaboration of the hydrosilylation mechanism and therefore the origin of the chemoselectivity are beyond the scope of this manuscript and will require more detailed mechanistic and computational studies. Nevertheless, (ⁱPrPNN^H)Fe(olefin) and (ⁱPrPDI)Fe(olefin) species might act as potential catalytic intermediates in the Fe-catalyzed alkene hydrosilylation,^{7a,29} and therefore we sought to compare at this point the relative ground state stabilization energies of alkene versus carbonyl binding for 5-hexen-2-one **11** to the (ⁱPrPNN^H)Fe-fragment³⁰ and the (ⁱPrPDI)Fe-fragment.

The enhanced electron-richness of the (PNN)Fe fragment (vide supra) should increase the binding affinity of the olefin functionality because of more favorable π -backbonding interactions. Similar to **21**, several spin configurations were considered, and their energies are compared in Figure 7. The differences between the (ⁱPrPNN^H)Fe and (ⁱPrPDI)Fe systems are striking. We find a dramatic stabilization of the carbonyl-bound species in the (PDI)Fe system, which is 11.9 kcal/mol more stable than the lowest olefin-bound isomer. In contrast, for the (PNN)Fe complex a clear preference for the olefin-bound isomer is observed, which is 4.1 kcal/mol more stable than the carbonyl-bound one (Figure 7). Overall, these results are consistent with the electrochemical observations, but steric effects will also effect the binding preferences to a certain extent and a comparison between the (ⁱPrPNN^H)Fe and (ⁱBuPNNⁱPr)Fe can be found in the SI.

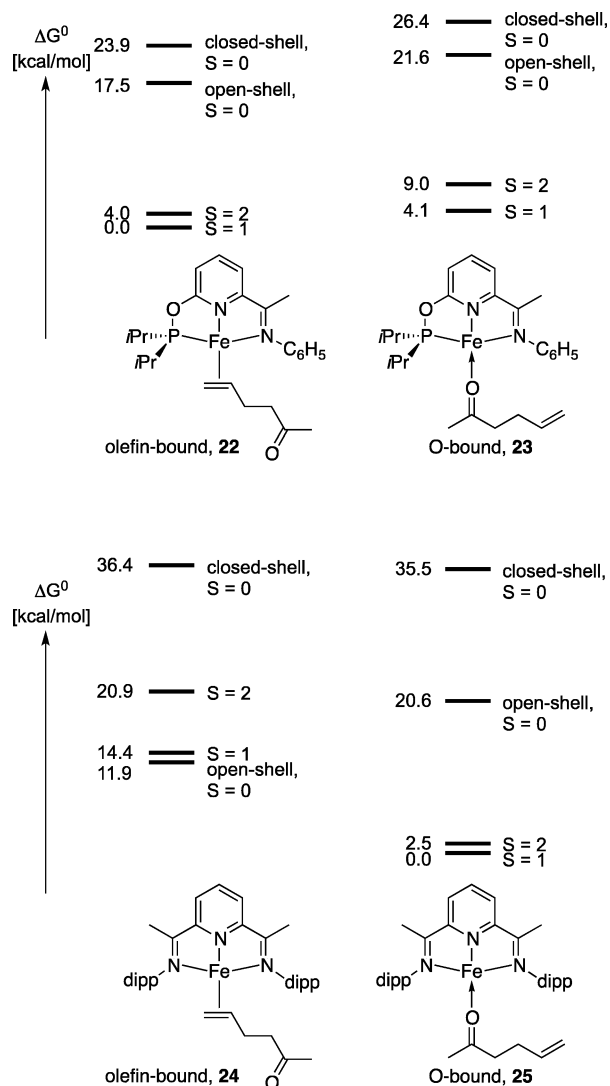


Figure 7. Free energy differences between the olefin-bound vs O-bound structures for the (ⁱPrPNN^H)Fe-fragment (top) and (ⁱPrPDI)Fe-fragment (bottom).

3. CONCLUDING REMARKS

We have prepared a series of iron pincer complexes ligated by phosphinite-iminopyridine ligands. Electrochemical measurements and IR spectroscopy indicate that these complexes are more electron-rich than the related (PDI)Fe complexes. Selective anti-Markovnikov alkene hydrosilylations with primary, secondary, and tertiary silanes have been achieved with these (PNN)Fe catalysts. Iron precursors with large substituents at both the P atom and 2,6-aryl positions are more effective than those with smaller substituents for alkene hydrosilylation with primary silanes, whereas the less sterically crowded iron precursors are highly active and selective for alkene hydrosilylation with secondary and tertiary silanes.

Although the (PNN)Fe catalysts are less efficient than Chirik's (PDI)Fe catalysts in hydrosilylation of simple α -olefins, successful hydrosilylations of alkenes bearing various functionalities, such as amide, ester, and ketone groups, highlight the remarkable chemoselectivity of the phosphinite-iminopyridine iron catalysts in alkenes hydrosilylation. These cost-effective and environmentally friendly iron hydrosilylation catalysts that are compatible with reactive functionalities provide distinct

advantages over traditional precious metal catalysts and previously reported iron catalysts for preparing functionalized alkylsilanes. Further investigations regarding the mechanistic implications of these observations are ongoing and will be reported in due course.

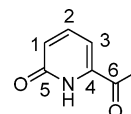
4. EXPERIMENTAL SECTION

General Considerations. All manipulations were performed under an argon or nitrogen atmosphere by using standard Schlenk techniques. All solvents were purified and dried according to standard methods prior to use. Diphenylsilane (98.0%), triethoxysilane (97.0%), and $(\text{Me}_3\text{SiO})_2\text{MeSiH}$ (98.0% MD'M) were purchased from TCI, and phenylsilane (98.0%) was purchased from J&K Scientific Ltd. All the silanes were used without further purification. Sodium hydride was purchased from Tianjin Beidouxing Fine Chemical Co., Ltd. and washed with pentane and dried under vacuum prior to use. Di-*tert*-butylchlorophosphine (96%) and chlorodiisopropylphosphine (96%) were purchased from Acros and used as received. Anhydrous iron(II) dichloride (98%) and iron(II) dibromide (98%) were purchased from Adamas and Aldrich, respectively, and used as received. NaHBEt_3 (1 M in toluene) was purchased from Aldrich and used as received. Hex-2-ene (85.0%) and pent-4-en-ol (98%) were purchased from Aldrich and used as received. 1-nitro-4-vinylbenzene (>95%) was purchased from J&K and used as received. 3-chloroprop-1-ene (>98%) was purchased from Shanghai Tianlian Fine Chemical Co., Ltd. and distilled from calcium hydride prior to use. 4-vinylbenzonitrile (98%) was purchased from Alfa Aesar and used as received. Cyclohexene (>99%) was purchased from Sinopharm chemical Reagent Co., Ltd. and distilled from calcium hydride prior to use. *n*-Octene ($\geq 98.0\%$) and 4-vinylpyridine (>96%) was purchased from Aladdin and distilled from calcium hydride prior to use. Styrene (99.0%), 4-methylstyrene (96.0%), 4-methoxystyrene (95.0%), 4-fluorostyrene (98.0%), 4-chlorostyrene (98.0%), but-3-en-1-ol (98%), allyl 3-oxobutanoate (>98%), 2-allylcyclohexanone ($\geq 98\%$), 4-vinylcyclohex-1-ene (95%), and 4-vinylphenyl acetate (98.0%) were purchased from TCI and used as received. Allyltrimethylsilane ($\geq 97\%$), allylbenzene ($\geq 98\%$) and 9-vinylcarbazole ($\geq 98\%$) were purchased from Adamas and used as received. Other alkenes including (1-(hex-5-en-1-yloxy)-2,2-dimethylpropane-1,1-diyl)dibenzene,³¹ hex-5-en-1-yl 4-methylbenzenesulfonate,³² *N*-allyl-*N*-benzylaniline,³³ ((pent-4-en-1-yloxy)methyl)benzene,³⁴ ((but-3-en-1-yloxy)methyl)benzene,³⁵ ((allyloxy)methyl)benzene,³⁶ 2-(but-3-en-1-yl)-2-methyl-1,3-dioxolane,³⁷ hex-5-en-1-yl benzoate,³⁸ and *N,N*-dimethylpent-4-enamide,³⁹ were synthesized according to the literature procedures. Compounds 1-(6-methoxypyridin-2-yl)ethanone,⁴⁰ 3-(4-fluoro-3-phenoxyphenyl)-1-propene,⁴¹ (4-methoxyphenyl)dimethylsilane,⁴² and *N*-allylbenzamide⁴³ were prepared according to the reported procedure. ¹H NMR spectra of **5a–h** were recorded on a Mercury (300 MHz) instrument. ¹H, ¹³C, and ³¹P NMR spectra of all the other compounds were recorded on Varian and Agilent instruments (400 MHz, 101 MHz, and 162 MHz respectively). The variable-temperature ¹H NMR were recorded on Agilent instrument (600 MHz). ¹H NMR chemical shifts were internally referenced to TMS (tetramethylsilane) signal or solvent residual signals. ¹³C NMR chemical shifts were internally referenced to solvent signals. ³¹P NMR chemical shifts were referenced to an external 85% H_3PO_4 standard. The ¹H NMR data of paramagnetic complexes are reported with the chemical shift, the peak width at half-height in Hertz, and integration value. Elemental analysis, infrared spectra, and high resolution mass spectra (HRMS) were collected by Analytical Laboratory of Shanghai Institute of Organic Chemistry (CAS).

Typical Procedure for Catalytic Hydrosilylation of Alkenes with Silanes. In a N_2 glovebox, a vial (10 mL) was charged with 1-octene (94 μL , 0.6 mmol), phenylsilane (74 μL , 0.6 mmol), dry toluene (1 mL), and complexes **5a** (6.0 μmol , 1 mol %). The reaction mixture was cooled to -34°C , and NaHBEt_3 (12 μmol , 2 mol %, 1 M in toluene) was then added to the reaction mixture. The resulting mixture was stirred for 3 h at room temperature. After that, the vial was removed from the glovebox, and the reaction mixture was

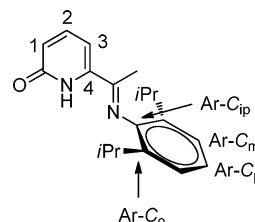
concentrated under dynamic vacuum. The residue was purified by flash chromatography, eluting with petrol ether to afford 124.0 mg of the desired product octyl(phenyl)silane **6** (0.56 mmol, 94%). ¹H NMR (400 MHz, CDCl_3) δ 7.55 (m, 2H), 7.39–7.33 (m, 3H), 4.27 (t, ³ $J_{\text{H,H}} = 3.6$ Hz, 2H, SiH_2), 1.47–1.43 (m, 2H, CH_2), 1.27–1.25 (m, 10H, CH_2), 0.96–0.93 (m, 2H, SiCH_2), 0.86 (t, ³ $J_{\text{H,H}} = 6.8$ Hz, 3H, CH_2Me); ¹³C{¹H} NMR (101 MHz, CDCl_3) δ 135.4, 133.0, 129.6, 128.1, 33.0 (Ar- CH_2), 32.1 (CH_2), 29.4 (CH_2), 29.3 (CH_2), 25.2 (CH_2), 22.8 (CH_2), 14.3 (CH_2Me), 10.2 (SiCH_2). These spectroscopic data agree with the reported data.⁴⁴

6-Acetylpyridin-2(1H)-one (2). In a 500 mL, single-neck flask was added 1-(6-methoxypyridin-2-yl)ethanone (10.0 g, 66.2 mmol, 1 equiv), 4 M HCl solution (90 mL, 396.9 mmol, 6 equiv), and 1,4-dioxane (200 mL). The reaction mixture was stirred at 80°C for 13 h. Then the solution was concentrated under reduced pressure. The residue was purified by flash chromatography on silica gel, eluting with dichloromethane/methanol 20:1 (v/v) to afford the title compound **2** as an off-white solid (9.1 g, 93% yield).



¹H NMR (400 MHz, D_2O) δ 7.73 (dd, ³ $J_{\text{H,H}} = 9.2$, ³ $J_{\text{H,H}} = 6.9$ Hz, 1H, 2-H), 7.27 (dd, ³ $J_{\text{H,H}} = 6.9$, ³ $J_{\text{H,H}} = 0.9$ Hz, 1H, 1- or 3-H), 6.80 (dd, ³ $J_{\text{H,H}} = 9.2$, ³ $J_{\text{H,H}} = 0.9$ Hz, 1H, 1- or 3-H), 2.55 (s, 3H, COMe); ¹³C{¹H} NMR (101 MHz, D_2O) δ 194.0 (C6), 163.9 (C5), 142.4 (C1, C2 or C3), 138.6 (C4), 125.7 (C1, C2 or C3), 113.2 (C1, C2 or C3), 24.5 (COMe). Anal. Calcd for $\text{C}_7\text{H}_7\text{NO}_2$: C, 61.31, H, 5.14, N, 10.21. Found: C, 61.16, H, 5.22, N, 10.27.

(E)-6-(1-(2,6-diisopropylphenyl)imino)ethylpyridin-2(1H)-one (3a). In a 100 mL single-neck flask was added 1-(6-hydroxypyridin-2-yl)ethanone (**2**) (2.0 g, 14.6 mmol, 1 equiv), 2,6-diisopropylaniline (3.9 g, 21.9 mmol, 1.5 equiv), *p*-tosyl acid (30.0 mg, 150 μmol , 1 mol %) and *n*-butanol (40 mL). After heating at reflux for 24 h with azeotropic removal of water using a Dean–Stark trap, the reaction mixture was concentrated under reduced pressure. The residue was purified by flash chromatography on silica gel eluting with dichloromethane/methanol 40:1 (v/v) to afford the title compound **3a** as a yellow solid (3.8 g, 89% yield).



¹H NMR (400 MHz, CDCl_3) δ 10.34 (s, 1H, NH), 7.50 (dd, ³ $J_{\text{H,H}} = 9.3$, ³ $J_{\text{H,H}} = 6.8$ Hz, 1H, 2-H), 7.18–7.11 (m, 3H, Ar-H), 6.77 (d, ³ $J_{\text{H,H}} = 9.3$ Hz, 1H, 1- or 3-H), 6.66 (d, ³ $J_{\text{H,H}} = 6.8$ Hz, 1H, 1- or 3-H), 2.62–2.51 (m, 2H, CHMe), 2.01 (s, 3H, $\text{N}=\text{CMe}$), 1.12 (d, ³ $J_{\text{H,H}} = 6.9$ Hz, 12H, CHMe_2); ¹³C{¹H} NMR (101 MHz, CDCl_3) δ 162.3 (N = C), 157.9 (C=O), 144.1 (Ar- C_{ip}), 140.5 (C4), 140.1 (C1, C2 or C3), 136.0 (Ar- C_o), 124.9 (Ar- C_p), 124.7 (Ar- C_m), 123.1 (C1, C2 or C3), 106.9 (C1, C2 or C3), 28.3 (CHMe_2), 23.3 (CHMe_2), 22.8 (CHMe_2), 15.8 ($\text{N}=\text{CMe}$). Anal. Calcd for $\text{C}_{19}\text{H}_{24}\text{N}_2\text{O}$: C, 76.99, H, 8.16, N, 9.45. Found: C, 76.75, H, 7.99, N, 9.31.

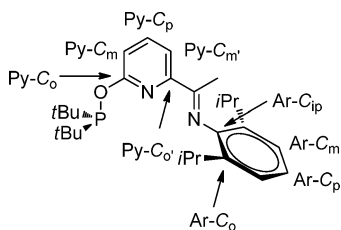
(E)-6-(1-(2,6-Diethylphenyl)imino)ethylpyridin-2(1H)-one (3b). In a 100 mL, single-neck flask was added 1-(6-hydroxypyridin-2-yl)ethanone (**2**) (2.0 g, 14.6 mmol, 1 equiv), 2,6-diethylaniline (3.3 g, 21.9 mmol, 1.5 equiv), *p*-tosylate acid (30.0 mg, 150 μmol , 1 mol %), and *n*-butanol (60 mL). After heating at reflux for 24 h with azeotropic removal of water using a Dean–Stark trap, the reaction mixture was concentrated under reduced pressure. The residue was purified by flash chromatography on silica gel, eluting with dichloromethane/methanol 40:1 (v/v) to afford the title compound **3b** as a yellow solid (3.7 g, 95% yield). ¹H NMR (400 MHz, CDCl_3) δ 10.34 (s, 1H), 7.49

(dd, $^3J_{\text{H,H}} = 9.3$, $^3J_{\text{H,H}} = 6.8$ Hz, 1H, 2-*H*), 7.12–7.05 (m, 3H, Ar-*H*), 6.76 (dd, $^3J_{\text{H,H}} = 9.2$, $^4J_{\text{H,H}} = 1.3$ Hz, 1H, 1- or 3-*H*), 6.66 (d, $^3J_{\text{H,H}} = 6.8$ Hz, 1H, 1- or 3-*H*), 2.35–2.20 (m, 4H, CH₂CH₃), 2.00 (s, 3H, N=CMe), 1.10 (t, $^3J_{\text{H,H}} = 7.5$ Hz, 6H, CH₂Me₂); $^{13}\text{C}\{^1\text{H}\}$ NMR (101 MHz, CDCl₃) δ 162.4 (C=N), 158.0 (C=O), 145.8 (Ar-C_{ip}), 140.8 (C4), 140.1 (C1, C2 or C3), 131.6 (Ar-C_o), 126.3 (Ar-C_p), 125.2 (Ar-C_m), 124.5 (C1, C2, or C3), 106.9 (C1, C2, or C3), 24.7 (CH₂CH₃), 15.8 (N = CMe), 14.0 (CH₂CH₃). Anal. Calcd for C₁₇H₂₀N₂O: C, 76.09, H, 7.51, N, 10.44. Found: C, 76.31, H, 7.66, N, 10.49.

(E)-6-(1-((2,6-Dimethylphenyl)imino)ethyl)pyridin-2(1H)-one (3c). In a 100 mL, single-neck flask was added 1-(6-hydroxypyridin-2-yl)ethanone (**2**) (2.0 g, 14.6 mmol, 1 equiv), 2,6-dimethylaniline (2.7 g, 21.9 mmol, 1.5 equiv), *p*-tosylate acid (30.0 mg, 150 μ mol, 1 mol %), and *n*-butanol (50 mL). After heating at reflux for 24 h with azeotropic removal of water using a Dean–Stark trap, the reaction mixture was concentrated under reduced pressure. The residue was purified by flash chromatography on silica gel, eluting with dichloromethane/methanol 40:1 (v/v) to afford the title compound **3c** as a yellow solid (3.6 g, 99% yield). ^1H NMR (400 MHz, CDCl₃) δ 10.35 (s, 1H, NH), 7.49 (dd, $^3J_{\text{H,H}} = 9.3$, $^3J_{\text{H,H}} = 6.8$ Hz, 1H, 2-*H*), 7.08–6.96 (m, 3H, Ar-*H*), 6.76 (dd, $^3J_{\text{H,H}} = 9.3$, $^4J_{\text{H,H}} = 1.4$ Hz, 1H, 1- or 3-*H*), 6.66 (d, $^3J_{\text{H,H}} = 6.8$ Hz, 1H, 1- or 3-*H*), 1.99 (s, 3H, N=CMe), 1.97 (s, 6H, Ar-Me); $^{13}\text{C}\{^1\text{H}\}$ NMR (101 MHz, CDCl₃) δ 162.3 (C=N), 157.9 (C=O), 146.8 (Ar-C_{ip}), 140.7 (C4), 140.1 (C1, C2 or C3), 128.1 (Ar-C_o), 125.6 (Ar-C_p), 125.1 (Ar-C_m), 124.0 (C1, C2 or C3), 106.9 (C1, C2 or C3), 18.0 (Ar-Me), 15.0 (N=CMe); Anal. Calcd for C₁₅H₁₆N₂O: C, 74.97, H, 6.71, N, 11.66. Found: C, 74.75, H, 6.72, N, 11.52.

(E)-6-(1-(Phenylimino)ethyl)pyridin-2(1H)-one (3d). In a 100 mL, single-neck flask was added 1-(6-hydroxypyridin-2-yl)ethanone (**2**) (2.0 g, 14.6 mmol, 1 equiv), aniline (2.0 mL, 21.9 mmol, 1.5 equiv), *p*-tosylate acid (30.0 mg, 150 μ mol, 1 mol %), and *n*-butanol (50 mL). After heating at reflux for 24 h with azeotropic removal of water using a Dean–Stark trap, the reaction mixture was concentrated under reduced pressure. The residue was purified by flash chromatography on silica gel, eluting with dichloromethane/methanol 30:1 (v/v) to afford the title compound **3d** as a brown solid (3.1 g, 87% yield). ^1H NMR (400 MHz, CDCl₃) δ 10.28 (s, 1H, NH), 7.47 (dd, $^3J_{\text{H,H}} = 9.2$, $^3J_{\text{H,H}} = 6.8$ Hz, 1H, 2-*H*), 7.38 (t, $^3J_{\text{H,H}} = 7.9$ Hz, 2H, Ar-*H_m*), 7.17 (t, $^3J_{\text{H,H}} = 7.5$ Hz, 1H, Ar-*H_p*), 6.79 (d, $^3J_{\text{H,H}} = 7.3$ Hz, 2H, Ar-*H_o*), 6.72 (d, $^3J_{\text{H,H}} = 9.1$ Hz, 1H, 1- or 3-*H*), 6.66 (d, $J = 6.8$ Hz, 1H, 1- or 3-*H*), 2.18 (s, 3H, N=CMe); $^{13}\text{C}\{^1\text{H}\}$ NMR (101 MHz, CDCl₃) δ 162.3 (N = C), 157.3 (C=O), 148.7 (Ar-C_{ip}), 141.3 (C4), 140.1 (C1, C2 or C3), 129.1 (Ar-C_o), 124.8 (Ar-C_p), 119.8 (Ar-C_m and C1, C2, or C3), 107.0 (C1, C2, or C3), 15.2 (N=CMe). Anal. Calcd for C₁₃H₁₂N₂O: C, 73.56, H, 5.70, N, 13.20. Found: C, 73.47, H, 5.65, N, 13.23.

***t*BuPNN^{ipr} Ligand, (E)-N-(1-(6-((Di-tert-butylphosphino)oxy)pyridin-2-yl)ethylidene)-2,6-diisopropylaniline (4a).**



Under an atmosphere of argon, NaH (158.0 mg, 6.3 mmol, 1.2 equiv) and THF (30 mL) were added to a 100 mL Schlenk tube. The solution of (E)-6-(1-((2,6-diisopropylphenyl)imino)ethyl)pyridin-2-ol (**3a**) (1.6 g, 5.3 mmol, 1 equiv) in THF (20 mL) was added dropwise to the Schlenk tube at room temperature. After that the mixture was stirred for 10 min, *t*Bu₂PCL (1.0 g, 5.5 mmol, 1.1 equiv) was added, and the resulting mixture was stirred for 3 h. The solvent was removed under vacuo, and then hexane (40 mL) was added. The resulting dark-yellow mixture was filtered through a pad of

Celite under Ar. The solvent was removed under reduced pressure to afford a yellow solid **4a** (2.2 g, 95% yield).

^1H NMR (400 MHz, CDCl₃) δ 8.00 (dd, $^3J_{\text{H,H}} = 7.5$, $^4J_{\text{P,H}} = 0.7$ Hz, 1H, Py-*H_m*), 7.71 (t, $^3J_{\text{H,H}} = 7.8$ Hz, 1H, Py-*H_p*), 7.16–7.06 (m, 3H, Ar-*H*), 6.97 (d, $^3J_{\text{H,H}} = 7.7$ Hz, 1H, Py-*H_m*), 2.79–2.68 (m, 2H, CHMe₂), 2.16 (s, 3H, N=CMe), 1.24 (d, $^3J_{\text{P,H}} = 11.6$ Hz, 18H, CMe₃), 1.13 (d, $^3J_{\text{H,H}} = 6.9$ Hz, 12H, CHMe₂); $^{31}\text{P}\{^1\text{H}\}$ NMR (162 MHz, CDCl₃) δ 155.9 (s); $^{13}\text{C}\{^1\text{H}\}$ NMR (101 MHz, CDCl₃) δ 167.1 (N = C), 164.0 (d, $^2J_{\text{P,C}} = 7.6$ Hz, Py-C_o), 154.7 (Py-C_o), 146.7 (Ar-C_{ip}), 139.3 (Py-C_p), 136.0 (Ar-C_o), 123.5 (Ar-C_p), 123.0 (Ar-C_m), 115.2 (Py-C_m), 113.8 (d, $^3J_{\text{P,C}} = 2.6$ Hz, Py-C_m), 35.8 (d, $^1J_{\text{P,C}} = 26.9$ Hz, CMe₃), 28.3 (CHMe₂), 27.8 (d, $^2J_{\text{P,C}} = 15.6$ Hz, CMe₃), 23.3 (CHMe₂), 23.0 (CHMe₂), 17.6 (N=CMe). HRMS (EI), *m/z* Calcd for C₂₇H₄₁N₂O⁺ (M⁺) 440.2957, found: 440.2968.

***t*BuPNN^{Et} Ligand, (E)-N-(1-(6-((Di-tert-butylphosphino)oxy)pyridin-2-yl)ethylidene)-2,6-diethylaniline (4b).** Under an atmosphere of argon, NaH (93.0 mg, 3.7 mmol, 1.2 equiv) and THF (10 mL) were added to a 100 mL Schlenk tube. The solution of (E)-6-(1-((2,6-diethylphenyl)imino)ethyl)pyridin-2-ol (**3b**) (840.0 mg, 3.1 mmol, 1 equiv) in THF (15 mL) was added dropwise to the Schlenk tube at room temperature. After that the mixture was stirred for 10 min, *t*Bu₂PCL (618.0 mg, 3.4 mmol, 1.1 equiv) was added, and the resulting mixture was stirred for 3 h. The solvent was removed under vacuo, hexane (30 mL) was added, and the dark-yellow mixture was filtered through a pad of Celite under Ar. The solvent was removed under reduced pressure to afford a yellow solid **4b** (1.2 g, 93% yield). ^1H NMR (400 MHz, CDCl₃) δ 8.00 (dd, $^3J_{\text{H,H}} = 7.5$, $^4J_{\text{P,H}} = 0.7$ Hz, 1H, Py-*H_m*), 7.70 (t, $^3J_{\text{H,H}} = 7.8$ Hz, 1H, Py-*H_p*), 7.10–7.00 (m, 3H, Ar-*H*), 6.96 (d, $^3J_{\text{H,H}} = 8$ Hz, 1H, Py-*H_m*), 2.44–2.26 (m, 4H, CH₂Me), 2.14 (s, 3H, N=CMe), 1.24 (d, $^3J_{\text{P,H}} = 11.6$ Hz, 18H, CMe₃), 1.13 (t, $^3J_{\text{H,H}} = 7.5$ Hz, 6H, CH₂Me); $^{31}\text{P}\{^1\text{H}\}$ NMR (162 MHz, CDCl₃) δ 156.0 (s); $^{13}\text{C}\{^1\text{H}\}$ NMR (101 MHz, CDCl₃) δ 167.1 (N = C), 164.0 (d, $^2J_{\text{P,C}} = 7.6$ Hz, Py-C_o), 154.7 (Py-C_o), 148.0 (Ar-C_{ip}), 139.3 (Py-C_p), 131.4 (Ar-C_o), 125.9 (Ar-C_m), 123.3 (Ar-C_p), 115.2 (Py-C_m), 113.8 (d, $^3J_{\text{P,C}} = 3.0$ Hz, Py-C_m), 35.7 (d, $^1J_{\text{P,C}} = 27.0$ Hz, CMe₃), 27.8 (d, $^2J_{\text{P,C}} = 15.6$ Hz, CMe₃), 24.7 (CH₂Me), 17.3 (N=CMe), 13.8 (CH₂Me). HRMS (ESI), *m/z* Calcd for C₂₅H₃₈N₂O⁺ (M + H)⁺ 413.2722, found: 413.2730.

***t*BuPNN^{Me} Ligand, (E)-N-(1-(6-((Di-tert-butylphosphino)oxy)pyridin-2-yl)ethylidene)-2,6-dimethylaniline (4c).** Under an atmosphere of argon, NaH (113.0 mg, 4.7 mmol, 1.1 equiv) and THF (10 mL) were added to a 100 mL Schlenk tube. The solution of (E)-6-(1-((2,6-dimethylphenyl)imino)ethyl)pyridin-2-ol (**3c**) (1.0 g, 4.3 mmol, 1 equiv) in THF (20 mL) was added dropwise to the Schlenk tube at room temperature. After that the mixture was stirred for 10 min, *t*Bu₂PCL (851.0 mg, 4.7 mmol, 1.1 equiv) was added, and the resulting mixture was stirred for 3 h. The solvent was removed under vacuo, hexane (30 mL) was added, and the dark-yellow mixture was filtered through a pad of Celite under Ar. The solvent was removed under reduced pressure to afford a yellow solid **4c** (1.6 g, 97% yield). ^1H NMR (400 MHz, CDCl₃) δ 8.03 (d, $^3J_{\text{H,H}} = 7.5$ Hz, 1H, Py-*H_m*), 7.71 (t, $^3J_{\text{H,H}} = 7.8$ Hz, 1H, Py-*H_p*), 7.07–6.91 (m, 4H, Ar-*H*, Py-*H_m*), 2.15 (s, 3H, N=CMe), 2.04 (s, 6H, Ar-Me), 1.25 (d, $J = 11.6$ Hz, 18H, CMe₃); $^{31}\text{P}\{^1\text{H}\}$ NMR (162 MHz, CDCl₃) δ 155.8 (s); $^{13}\text{C}\{^1\text{H}\}$ NMR (101 MHz, CDCl₃) δ 167.4 (N = C), 163.9 (d, $^2J_{\text{P,C}} = 7.7$ Hz, Py-C_o), 154.7 (Py-C_o), 148.9 (Ar-C_{ip}), 139.4 (Py-C_p), 127.9 (Ar-C_o), 125.6 (Ar-C_p), 123.0 (Ar-C_m), 115.2 (Py-C_m), 113.8 (d, $^3J_{\text{P,C}} = 2.5$ Hz, Py-C_m), 35.7 (d, $^1J_{\text{P,C}} = 26.8$ Hz, CMe₃), 27.7 (d, $^2J_{\text{P,C}} = 15.6$ Hz, CMe₃), 18.1 (Ar-Me), 17.0 (N=CMe). HRMS (EI), *m/z* Calcd for C₂₃H₃₃N₂O⁺ (M⁺) 384.2331, found: 384.2327.

***t*BuPNN^H Ligand, (E)-N-(1-(6-((Di-tert-butylphosphino)oxy)pyridin-2-yl)ethylidene)aniline (4d).** Under an atmosphere of argon, NaH (130.0 mg, 5.4 mmol, 1.1 equiv) and THF (10 mL) were added to a 100 mL Schlenk tube. The solution of (E)-6-(1-(phenylimino)ethyl)pyridin-2-ol (**3d**) (1.0 g, 4.9 mmol, 1 equiv) in THF (20 mL) was added dropwise to the Schlenk tube at room temperature. After that the mixture was stirred for 10 min, *t*Bu₂PCL (972.0 mg, 5.4 mmol, 1.1 equiv) was added, and the resulting mixture was stirred for 3 h. The solvent was removed under vacuo, hexane (30 mL) was added, and the brown mixture was filtered through a pad of Celite under Ar. The

solvent was removed under reduced pressure to afford an orange oil **4d** (1.5 g, 88% yield). NMR spectra: ^1H NMR (400 MHz, CDCl_3) δ 7.89 (dd, $^3J_{\text{H,H}} = 7.5$ Hz, $^4J_{\text{P,H}} = 0.7$ Hz, 1H, Py- H_m), 7.60 (t, $^3J_{\text{H,H}} = 8$ Hz, 1H, Py- H_p), 7.37–7.26 (m, 2H, Ar- H_o), 7.12–7.07 (m, 1H, Ar- H_p), 6.94 (d, $^3J_{\text{H,H}} = 8.1$ Hz, 1H, Py- H_m), 6.82–6.79 (m, 2H, Ar- H_m), 2.31 (s, 3H, N=CMe), 1.23 (d, $^3J_{\text{P,H}} = 11.7$ Hz, 18H, CMe₃); $^{31}\text{P}\{^1\text{H}\}$ NMR (162 MHz, CDCl_3) δ 155.4 (s); $^{13}\text{C}\{^1\text{H}\}$ NMR (101 MHz, CDCl_3) δ 167.7 (N = C), 163.9 (d, $^2J_{\text{P,C}} = 7.6$ Hz, Py- C_o), 155.1 (Py- C_o), 151.5 (Ar- C_{ip}), 139.3 (Py- C_p), 129.0 ((Ar- C_o)), 123.5 (Ar- C_p), 119.4 (Ar- C_m), 115.3 (Py- C_m), 113.8 (d, $^3J_{\text{P,C}} = 2.3$ Hz, Py- C_m), 35.7 (d, $^1J_{\text{P,C}} = 27.0$ Hz, CMe₃), 27.7 (d, $^2J_{\text{P,C}} = 15.7$ Hz, CMe₃), 16.8 (N=CMe). HRMS (EI), m/z Calcd for $\text{C}_{21}\text{H}_{29}\text{N}_2\text{OP}$ (M^+) 356.2018, found: 356.2023.

$^{ipr}\text{PNN}^{Pr}$ Ligand, (E)-N-(1-(6-((Diisopropylphosphino)oxy)pyridin-2-yl)ethylidene)-2,6-diisopropylaniline (**4e**). Under an atmosphere of argon, NaH (71.0 mg, 3.0 mmol, 1.1 equiv) and THF (15 mL) were added to a 100 mL Schlenk tube. The solution of (E)-6-(1-((2,6-diisopropylphenyl)imino)ethyl)pyridin-2-ol (**3a**) (0.8 g, 2.7 mmol, 1 equiv) in THF (10 mL) was added dropwise to the Schlenk tube at room temperature. After that the mixture was stirred for 10 min, $i\text{Pr}_2\text{PCl}$ (450 mg, 3.0 mmol, 1.1 equiv) was added, and the resulting mixture was stirred for 3 h. The solvent was removed under vacuo, hexane (30 mL) was added, and the dark-yellow mixture was filtered through a pad of Celite under Ar. The solvent was removed under reduced pressure to afford a yellow solid **4e** (1.0 g, 92% yield). ^1H NMR (400 MHz, CDCl_3) δ 7.99 (dd, $^3J_{\text{H,H}} = 7.5$ Hz, $^4J_{\text{P,H}} = 0.7$ Hz, 1H, Py- H_m), 7.70 (t, $^3J_{\text{H,H}} = 7.8$ Hz, 1H, Py- H_p), 7.16–7.06 (m, 3H, Ar- H), 6.92 (d, $^3J_{\text{H,H}} = 8.1$ Hz, 1H, Py- H_m), 2.79–2.69 (m, 2H, CHMe₂), 2.18 (s, 3H, N=CMe), 2.10–1.99 (m, 2H, CHMe₂), 1.24–1.10 (m, 24H, CHMe₂); $^{31}\text{P}\{^1\text{H}\}$ NMR (162 MHz, CDCl_3) δ 146.8 (s); $^{13}\text{C}\{^1\text{H}\}$ NMR (101 MHz, CDCl_3) δ 166.9 (N = C), 163.4 (d, $^2J_{\text{P,C}} = 6.1$ Hz, Py- C_o), 154.6 (d, $^4J_{\text{P,C}} = 1.1$ Hz, Py- C_o), 146.7 (Ar- C_{ip}), 139.3 (d, $^3J_{\text{P,C}} = 1.9$ Hz, Py- C_m), 136.0 (Ar- C_o), 123.6 (Ar- C_p), 123.1 (Ar- C_m), 115.1 (Py- C_m), 113.5 (d, $^4J_{\text{P,C}} = 0.8$ Hz, Py- C_p), 28.3 (CHMe₂), 28.1 (d, $^1J_{\text{P,C}} = 19.1$ Hz, PCH), 23.3 (CHMe₂), 23.0 (CHMe₂), 18.1 (d, $^2J_{\text{P,C}} = 20.6$ Hz, PCHMe₂), 17.6 (N=CMe), 17.5 (d, $^2J_{\text{P,C}} = 9.7$ Hz, PCHMe₂). HRMS (ESI), m/z Calcd for $\text{C}_{25}\text{H}_{37}\text{N}_2\text{OP}$ ($M + \text{H}^+$) 413.2722, found: 413.2716.

$^{ipr}\text{PNN}^{Et}$ Ligand, (E)-N-(1-(6-((Diisopropylphosphino)oxy)pyridin-2-yl)ethylidene)-2,6-diethylylaniline (**4f**). Under an atmosphere of argon, NaH (120.0 mg, 5.0 mmol, 1.1 equiv) and THF (20 mL) were added to a 100 mL Schlenk tube. The solution of (E)-6-(1-((2,6-diethylphenyl)imino)ethyl)pyridin-2-ol (**3b**) (1.2 g, 4.6 mmol, 1 equiv) in THF (30 mL) was added dropwise to the Schlenk tube at room temperature. After that the mixture was stirred for 10 min, $i\text{Pr}_2\text{PCl}$ (763.0 mg, 5.0 mmol, 1.1 equiv) was added, and the resulting mixture was stirred for 3 h. The solvent was removed under vacuo, hexane (30 mL) was added, and the dark-yellow mixture was filtered through a pad of Celite under Ar. The solvent was removed under reduced pressure to afford a yellow solid **4f** (1.5 g, 87% yield). ^1H NMR (400 MHz, CDCl_3) δ 7.99 (d, $^3J_{\text{H,H}} = 7.5$ Hz, 1H, Py- H_m), 7.69 (t, $^3J_{\text{H,H}} = 7.8$ Hz, 1H, Py- H_p), 7.11–6.99 (m, 3H, Ar- H), 6.92 (d, $^3J_{\text{H,H}} = 8.1$ Hz, 1H, Py- H_m), 2.44–2.27 (m, 4H, CH₂Me), 2.16 (s, 3H, N=CMe), 2.10–1.98 (m, 2H, CHMe₂), 1.23–1.11 (m, 18H, CH₂Me, CHMe₂); $^{31}\text{P}\{^1\text{H}\}$ NMR (162 MHz, CDCl_3) δ 146.9 (s); $^{13}\text{C}\{^1\text{H}\}$ NMR (101 MHz, CDCl_3) δ 166.9 (N = C), 163.4 (d, $^2J_{\text{P,C}} = 6.1$ Hz, Py- C_o), 154.6 (d, $^4J_{\text{P,C}} = 1.2$ Hz, Py- C_o), 148.0 (Ar- C_{ip}), 139.3 (d, $^4J_{\text{P,C}} = 1.2$ Hz, Py- C_p), 131.4 (Ar- C_o), 126.0 (Ar- C_p), 123.3 (Ar- C_m), 115.1 (Py- C_m), 113.5 (d, $^3J_{\text{P,C}} = 1.9$ Hz, Py- C_m), 28.1 (d, $^1J_{\text{P,C}} = 19.1$ Hz, PCH), 24.7 (CH₂Me), 18.2 (d, $^2J_{\text{P,C}} = 20.4$ Hz, CHMe₂), 17.6 (M = CMe), 17.4 (d, $^2J_{\text{P,C}} = 21.2$ Hz, CHMe₂), 13.8 (CH₂Me). HRMS (EI), m/z Calcd for $\text{C}_{21}\text{H}_{29}\text{N}_2\text{OP}$ (M^+) 356.2018, found: 356.2021.

$^{ipr}\text{PNN}^{Me}$ Ligand, (E)-N-(1-(6-((Diisopropylphosphino)oxy)pyridin-2-yl)ethylidene)-2,6-dimethylylaniline (**4g**). Under an atmosphere of argon, NaH (144.0 mg, 6.0 mmol, 1.1 equiv) and THF (20 mL) were added to a 100 mL Schlenk tube. The solution of (E)-6-(1-((2,6-dimethylphenyl)imino)ethyl)pyridin-2-ol (**3c**) (1.3 g, 5.5 mmol, 1 equiv) in THF (30 mL) was added dropwise to the Schlenk tube at room temperature. After that the mixture was stirred for 10 min, $i\text{Pr}_2\text{PCl}$ (920.0 mg, 6.0 mmol, 1.1 equiv) was added, and the resulting

mixture was stirred for 3 h. The solvent was removed under vacuo, hexane (40 mL) was added, and the dark-yellow mixture was filtered through a pad of Celite under Ar. The solvent was removed under reduced pressure to afford a yellow solid **4g** (1.8 g, 99% yield). ^1H NMR (400 MHz, CDCl_3) δ 8.00 (d, $^3J_{\text{H,H}} = 7.5$ Hz, 1H, Py- H_m), 7.69 (t, $^3J_{\text{H,H}} = 7.8$ Hz, 1H, Py- H_p), 7.06–6.90 (m, 4H, Py- H_m , Ar- H), 2.15 (s, 3H, N=CMe), 2.02 (s, 6H, Ar- Me), 1.16–1.07 (m, 14H, PCH, CHMe₂); $^{31}\text{P}\{^1\text{H}\}$ NMR (162 MHz, CDCl_3) δ 146.7 (s); $^{13}\text{C}\{^1\text{H}\}$ NMR (101 MHz, CDCl_3) δ 167.2 (N = C), 163.3 (d, $^2J_{\text{P,C}} = 6.1$ Hz, Py- C_o), 154.5 (d, $^4J_{\text{P,C}} = 1.2$ Hz, Py- C_o), 148.9 (Ar- C_{ip}), 139.3 (d, $^4J_{\text{P,C}} = 1.1$ Hz, Py- C_p), 127.9 (Ar- C_o), 125.6 (Ar- C_p), 123.0 (Ar- C_m), 115.1 (Py- C_m), 113.6 (d, $^3J_{\text{P,C}} = 1.9$ Hz, Py- C_m), 28.0 (d, $^1J_{\text{P,C}} = 18.8$ Hz, CHMe₂), 18.1 (d, $^2J_{\text{P,C}} = 20.6$ Hz, PCH), 18.0 (Ar- Me), 17.5 (d, $^2J_{\text{P,C}} = 9.3$ Hz, CHMe₂), 16.9 (N=CMe). HRMS (EI), m/z Calcd for $\text{C}_{21}\text{H}_{29}\text{N}_2\text{OP}$ (M^+) 356.2018, found: 356.2021.

$^{ipr}\text{PNN}^{Et}$ Ligand, (E)-N-(1-(6-((Diisopropylphosphino)oxy)pyridin-2-yl)ethylidene)aniline (**4h**). Under an atmosphere of argon, NaH (84.0 mg, 3.5 mmol, 1.1 equiv) and THF (10 mL) were added to a 100 mL Schlenk tube. The solution of (E)-6-(1-(phenylimino)ethyl)pyridin-2-ol (**3d**) (676.0 mg, 3.2 mmol, 1 equiv) in THF (20 mL) was added dropwise to the Schlenk tube at room temperature. After that the mixture was stirred for 10 min, $i\text{Pr}_2\text{PCl}$ (534.0 mg, 3.5 mmol, 1.1 equiv) was added, and the resulting mixture was stirred for 3 h. The solvent was removed under vacuo, hexane (25 mL) was added, and the brown mixture was filtered through a pad of Celite under Ar. The solvent was removed under reduced pressure to afford an orange oil **4h** (910.0 mg, 87% yield). ^1H NMR (400 MHz, CDCl_3) δ 7.89 (d, $^3J_{\text{H,H}} = 7.5$ Hz, 1H, Py- H_m), 7.67 (t, $^3J_{\text{H,H}} = 7.8$ Hz, 1H, Py- H_p), 7.35 (t, $^3J_{\text{H,H}} = 7.8$ Hz, 2H, Ar- H_m), 7.09 (t, $^3J_{\text{H,H}} = 7.4$ Hz, 1H, Ar- H_p), 6.89 (d, $^3J_{\text{H,H}} = 8.1$ Hz, 1H, Py- H_m), 6.80 (d, $^3J_{\text{H,H}} = 7.6$ Hz, 2H, Ar- H_o), 2.32 (s, 3H, N=CMe), 2.13–1.87 (m, 2H, CHMe₂), 1.22–1.13 (m, 12H, CHMe₂); $^{31}\text{P}\{^1\text{H}\}$ NMR (162 MHz, CDCl_3) δ 146.5 (s); $^{13}\text{C}\{^1\text{H}\}$ NMR (101 MHz, CDCl_3) δ 167.3 (N = C), 163.2 (d, $^2J_{\text{P,C}} = 6.1$ Hz, Py- C_o), 154.9 (d, $^4J_{\text{P,C}} = 1.1$ Hz, Py- C_o), 151.5 (Ar- C_{ip}), 139.3 (Py- C_p), 129.0 (Ar- C_o), 123.5 (Ar- C_p), 119.3 (Ar- C_m), 115.2 (Py- C_m), 113.5 (d, $^3J_{\text{P,C}} = 1.6$ Hz, Py- C_m), 28.0 (d, $^1J_{\text{P,C}} = 19.1$ Hz, CHMe₂), 18.1 (d, $^2J_{\text{P,C}} = 20.5$ Hz, CHMe₂), 17.5 (d, $^2J_{\text{P,C}} = 9.3$ Hz, CHMe₂), 16.7 (N=CMe). HRMS (EI), m/z Calcd for $\text{C}_{19}\text{H}_{25}\text{N}_2\text{OP}$ (M^+) 328.1705, found: 328.1708.

$^{tBu}\text{PNN}^{ipr}\text{FeCl}_2$ (**5a**). In a N_2 -filled glovebox, ligand **4a** (1.2 g, 2.8 mmol) was added to a solution of FeCl_2 (350.0 mg, 2.8 mmol) in THF (60 mL) at room temperature with vigorous stirring. The colorless solution turned to a dark-blue suspension immediately. After being stirred at room temperature for 24 h, the solution was reduced to about 10 mL via evaporation under vacuo. Then the suspension was filtered, and the resulting solid was washed with 20 mL ether and dried under vacuo. The product was obtained as a dark-blue powder (1.4 g, 90% yield). The complex **5a** was dissolved in a mixture of dichloromethane and tetrahydrofuran. The solvent evaporated slowly at room temperature in the N_2 -filled glovebox. After a few days, dark-green crystals of complex **5a** were obtained for X-ray analysis. ^1H NMR (300 MHz, CD_2Cl_2) δ 87.5 (81.9, 1H), 59.1 (78.4, 1H), 58.0 (49.7, 1H), 11.2 (118.0, 18H, CMe₃), 8.1 (34.0, 3H, N=CMe), 3.1 (22.0, 12H, CHMe₂), –5.93 (7.0, 1H), –10.9 (65.2, 2H, CHMe₂), –12.0 (31.0, 1H), –12.5 (34.6, 1H). Anal. Calcd for $\text{C}_{27}\text{H}_{41}\text{Cl}_2\text{FeN}_2\text{OP}$: C, 57.16, H, 7.28, N, 4.94. Found: C, 57.32, H, 7.42, N, 6.68. μ_{eff} (Evan's method, CDCl_3 , 25 °C) = 5.3 μ_B .

$^{tBu}\text{PNN}^{Et}\text{FeBr}_2$ (**5b**). In a N_2 -filled glovebox, ligand **4b** (654.0 mg, 1.6 mmol, 1 equiv) was added to a solution of FeBr_2 (342.0 mg, 1.6 mmol, 1 equiv) in THF (50 mL) at room temperature with vigorous stirring. The orange solution turned to dark blue immediately. Then the reaction flask was sealed and heated in an oil bath. After being stirred at 80 °C for 16 h, the reaction solution was cooled to room temperature. The solvent was removed under vacuo. Then 10 mL ether was added, and the resulting suspension was filtered. The solid was washed with 10 mL ether and dried in vacuo. The product was obtained as a gray powder (880.0 mg, 88% yield). ^1H NMR (300 MHz, CD_2Cl_2) δ 85.2 (8.9, 1H), 61.6 (72.3, 2H), 55.3 (45.4, 1H), 13.6 (114.1, 18H, CMe₃), 8.7 (27.2, 3H, N=CMe), 1.2 (17.1, 4H, CH₂Me), –1.0 (34.0, 6H, CH₂Me), –13.6 (24.5, 1H), –15.2 (38.5,

1H). Anal. Calcd for $C_{25}H_{37}Br_2FeN_2OP$: C, 47.80, H, 5.94, N, 4.46. Found: C, 47.90, H, 6.02, N, 4.50. μ_{eff} (Evan's method, $CDCl_3$, 25 °C) = 5.3 μ_B .

(^{tBu}PNN^{Me})FeBr₂ (**5c**). In a N₂-filled glovebox, ligand **4c** (638.0 mg, 1.7 mmol, 1 equiv) was added to a solution of FeBr₂ (358.0 mg, 1.7 mmol, 1 equiv) in THF (100 mL) at room temperature with vigorous stirring. The orange solution turned to dark blue immediately. Then the reaction flask was sealed and heated in an oil bath. After being stirred at 80 °C for 17 h, the reaction solution was cooled to room temperature. The solvent was removed under vacuo. Then ether (10 mL) was added, and the resulting suspension was filtered. The solid was washed with 10 mL ether and dried in vacuo. The product was obtained as a brown powder (860.0 mg, 86% yield). ¹H NMR (300 MHz, CD₂Cl₂) δ 84.8 (63.8, 1H), 60.8 (60.7, 1H), 55.8 (36.2, 1H), 14.0 (103.5, 18H, CMe₃), 11.8 (108.6, 3H, N=CMe), 9.3 (22.8, 1H), 4.1 (60.5, 3H, Ar-Me), 2.0 (18.6, 3H, Ar-Me), -13.9 (21.7, 1H), -16.4 (25.3, 1H). Anal. Calcd for $C_{23}H_{33}Br_2FeN_2OP$: C, 46.03, H, 5.54, N, 4.67. Found: C, 45.76, H, 5.62, N, 4.73. μ_{eff} (Evan's method, $CDCl_3$, 25 °C) = 5.6 μ_B .

(^{tBu}PNN^{Pr})FeBr₂ (**5d**). In a N₂-filled glovebox, ligand **4d** (808.0 mg, 2.3 mmol, 1 equiv) was added to a solution of FeBr₂ (488.0 mg, 2.3 mmol, 1 equiv) in THF (100 mL) at room temperature with vigorous stirring. The orange solution turned to dark blue immediately. Then the reaction flask was sealed and heated in an oil bath. After being stirred at 80 °C for 15 h, the reaction solution was cooled to room temperature. The solvent was removed under vacuo. Then ether (10 mL) was added, and the resulting suspension was filtered. The solid was washed with 10 mL ether and dried under vacuo. The product was obtained as a brown powder (1.1 g, 85% yield). ¹H NMR (300 MHz, CD₂Cl₂) δ 81.8 (56.9, 2H), 57.6 (29.9, 1H), 42.0 (55.9, 2H), 15.8 (106.8, 18H, CMe₃), 13.0 (22.7, 3H, N=CMe), -6.8 (128.8, 1H), -10. Nine (20.7, 1H), -22.7 (28.6, 1H). Anal. Calcd for $C_{21}H_{29}Br_2FeN_2OP$: C, 44.09, H, 5.11, N, 4.90. Found: C, 43.98, H, 5.39, N, 5.03. μ_{eff} (Evan's method, $CDCl_3$, 25 °C) = 5.6 μ_B .

(^{iPr}PNN^{iPr})FeBr₂ (**5e**). In a N₂-filled glovebox, ligand **4e** (850.0 mg, 2.1 mmol, 1 equiv) was added to a solution of FeBr₂ (440.0 mg, 2.1 mmol, 1 equiv) in THF (100 mL) at room temperature with vigorous stirring. The colorless solution turned to dark-blue suspension immediately. After being stirred at room temperature for 24 h, the volume of solution was reduced to about 15 mL via evaporation under vacuo. Then the suspension was filtered, and the resulting solid was washed with 15 mL ether and dried under vacuo. The product was obtained as gray powder (1.2 g, 93% yield). The ¹H NMR spectrum of complex **5e** could not be obtained due to its poor solubility in common organic solvents. Anal. Calcd for $C_{25}H_{37}Br_2FeN_2OP$: C, 47.80, H, 5.94, N, 4.46. Found: C, 47.95, H, 6.16, N, 4.28.

(^{iPr}PNN^{Et})FeBr₂ (**5f**). In a N₂-filled glovebox, ligand **4f** (1.0 g, 2.6 mmol, 1 equiv) was added to the solution of FeBr₂ (560.0 mg, 2.6 mmol, 1 equiv) in THF (100 mL) at room temperature with vigorous stirring. The orange solution turned to dark blue immediately. Then the reaction flask was sealed and heated in an oil bath. After being stirred at 80 °C for 25 h, the reaction solution was cooled to room temperature. The solvent was removed under vacuo. Then ether (20 mL) was added, and the resulting suspension was filtered. The solid was washed with 10 mL ether and dried under vacuo. The product was obtained as a brown powder (1.3 g, 83% yield). ¹H NMR (300 MHz, CD₂Cl₂) δ 130.6 (154.6, 2H), 83.2 (63.4, 1H), 69.1 (66.7, 2H, CHMe₂), 53.1 (38.2, 1H), 16.7 (136.0, 3H, N=CMe), 10.2 (28.4, 12H, CHMe₂), 7.1 (166.7, 1H), 3.6 (77.7, 4H, CH₂Me), -0.5 (26.8, 6H, CH₂Me), -12.4 (17.2, 1H), -13.0 (26.9, 1H). Anal. Calcd for $C_{23}H_{33}Br_2FeN_2OP$: C, 46.03, H, 5.54, N, 4.67. Found: C, 45.99, H, 5.69, N, 4.68. μ_{eff} (Evan's method, $CDCl_3$, 25 °C) = 5.6 μ_B .

(^{iPr}PNN^{Me})FeBr₂ (**5g**). In a N₂-filled glovebox, ligand **4g** (886.0 mg, 2.5 mmol, 1 equiv) was added to the solution of FeBr₂ (536.0 mg, 2.5 mmol, 1 equiv) in THF (100 mL) at room temperature with vigorous stirring. The colorless solution turned to dark blue immediately. Then the reaction flask was sealed and heated in an oil bath. After being stirred at 80 °C for 1 h, dark-blue solid precipitated from the solution. After being stirred for another 18 h at 80 °C, the reaction mixture was cooled to room temperature, and the volume of solution was reduced

to about 5 mL via evaporation under vacuo. Then the suspension was filtered, and the resulting solid was washed with 15 mL ether and dried under vacuo. The product was obtained as a dark-blue powder (1.4 g, 95% yield). ¹H NMR (300 MHz, CD₂Cl₂) δ 133.4 (161.7, 1H), 82.9 (68.6, 2H), 68.3 (74.8, 2H), 53.5 (35.3, 1H), 13.9 (107.1, 6H, CHMe₂), 10.8 (20.5, 3H, N=CMe), 10.3 (93.4, 6H, CHMe₂), 4.56 (78.6, 6H, Ar-Me), -12.9 (18.5, 1H), -15.4 (30.7, 1H). Anal. Calcd for $C_{21}H_{29}Br_2FeN_2OP$: C, 44.09, H, 5.11, N, 4.90. Found: C, 44.11, H, 5.18, N, 4.9. μ_{eff} (Evan's method, $CDCl_3$, 25 °C) = 5.6 μ_B .

(^{iPr}PNN^H)FeBr₂ (**5h**). In a N₂-filled glovebox, ligand **4h** (720.0 mg, 2.2 mmol, 1 equiv) was added to the solution of FeBr₂ (470.0 mg, 2.2 mmol, 1 equiv) in THF (50 mL) at room temperature with vigorous stirring. The orange solution turned to dark blue immediately. Then the reaction flask was sealed and heated in an oil bath. After being stirred at 80 °C for 18 h, the reaction solution was cooled to room temperature. The solvent was removed in vacuo. Then ether (15 mL) was added, and the resulting suspension was filtered. The solid was washed with 10 mL ether and dried in vacuo. The product was obtained as a brown powder (1.1 g, 92% yield). The complex **5h** was dissolved in dichloromethane and the solvent evaporated slowly at room temperature in the N₂-filled glovebox. After a few days, dark-red crystals of **5h** were obtained suitable for X-ray analysis. ¹H NMR (300 MHz, CD₂Cl₂) δ 137.2 (172.2, 1H), 76.3 (53.7, 2H), 56.1 (28.7, 1H), 47.8 (65.1, 2H, CHMe₂), 14.3 (92.0, 6H, CHMe₂), 14.0 (22.6, 3H, N=CMe), 7.9 (74.1, 6H, CHMe₂), -1.7 (149.3, 2H), -8.7 (17.3, 1H), -27.2 (26.3, 1H). Anal. Calcd for $C_{19}H_{25}Br_2FeN_2OP$: C, 41.95, H, 4.63, N, 5.15. Found: C, 41.86, H, 4.92, N, 5.05. μ_{eff} (Evan's method, $CDCl_3$, 25 °C) = 5.1 μ_B .

Silafluofen (**19**). In N₂-filled glovebox, a vial (10 mL) was charged with 4-allyl-1-fluoro-2-phenoxybenzene (**17**) (114.0 mg, 0.5 mmol), dimethyl(4-propylphenyl)silane (**18**) (106.9 mg, 0.6 mmol), complex **5h** (50.0 μ mol, 10 mol %), and dry toluene (0.9 mL). The reaction mixture was cooled to -34 °C and NaBHET₃ (100 μ L, 20 mol %, 1 M in toluene) was then added to the mixture. The reaction mixture was stirred at room temperature for 5 d. The vial was then removed from the glovebox. The mixture was filtered through a pad of silica gel, and the solvent was removed under vacuo. The desired product was obtained as colorless oil by flash chromatography on silica gel, eluting with petrol ether/ethyl acetate (v/v = 100:1) (113.0 mg, 55% yield). ¹H NMR (300 MHz, CDCl₃) δ 7.39–7.29 (m, 4H), 7.11–7.03 (m, 2H), 7.00 (d, ³J_{H,H} = 8.1 Hz, 2H), 6.90–6.83 (m, 4H), 4.03 (q, ³J_{H,H} = 7.0 Hz, 2H, OCH₂Me), 2.54 (t, ³J_{H,H} = 7.5 Hz, 2H, CH₂), 1.63–1.52 (m, 2H, CH₂), 1.42 (t, ³J_{H,H} = 7.0 Hz, 3H, OCH₂Me), 0.74–0.68 (m, 2H, CH₂), 0.22 (s, 6H, SiMe₂); ¹⁹F NMR (282 MHz, CDCl₃) δ -135.7 (m); ¹³C NMR (101 MHz, CDCl₃) δ 159.8, 157.7, 152.7 (d, ¹J_{F,C} = 246.1 Hz), 143.0 (d, ²J_{F,C} = 11.6 Hz), 139.5 (d, ³J_{F,C} = 3.8 Hz), 135.1, 129.9, 129.8, 124.9 (d, ³J_{F,C} = 6.6 Hz), 123.0, 122.1, 117.1, 116.7 (d, ²J_{F,C} = 18.1 Hz), 114.2, 63.3 (OCH₂Me), 39.0 (CH₂), 26.0 (CH₂), 15.7, 15.0, -2.8 (SiMe₂). These spectroscopic data agree with the reported data.⁴⁵

(^{tBu}PNN^{iPr})Fe(CO)₂ (**21**). In a N₂-filled glovebox, a thick-walled reaction vessel (100 mL) was charged with complex **5a** (307 mg, 0.54 mmol) and dry toluene (50 mL). The reaction mixture was cooled to -34 °C, and NaBHET₃ (1 mL, 1.0 mmol, 1 M in toluene) was added to the mixture. The mixture was stirred for about 5 min. Then the vessel was transferred from the glovebox, and the reaction mixture was frozen to liquid nitrogen temperature. The vessel was evacuated, and CO was added. The resulting mixture was warmed to room temperature and stirred for 7 h. The solvent was removed under vacuo. Pentane (50 mL) was then added, and the solution was filtered through Celite. The solvent was removed under vacuo, and the resulting dark-green solid was recrystallized in pentane to yield 153.0 mg (51%) of **21**. The complex **21** was dissolved in ether. The solvent evaporated slowly at room temperature in the N₂-filled glovebox. After a few days, dark-green crystals of complex **21** were obtained suitable for X-ray analysis.

- Ed.* **2008**, 47, 2497. (f) Tondreau, A. M.; Darmon, J. M.; Wile, B. M.; Floyd, S. K.; Lobkovsky, E.; Chirik, P. J. *Organometallics* **2009**, 28, 3928. (g) Addis, D.; Shaikh, N.; Zhou, S.; Das, S.; Junge, K.; Beller, M. *Chem.—Asian J.* **2010**, 5, 1687. (h) Inagaki, T.; Ito, A.; Ito, J.-i.; Nishiyama, H. *Angew. Chem., Int. Ed.* **2010**, 49, 9384. (i) Kandepe, V. V. K. M.; Cardoso, J. M. S.; Peris, E.; Royo, B. *Organometallics* **2010**, 29, 2777. (j) Inagaki, T.; Phong, L. T.; Furuta, A.; Ito, J.-i.; Nishiyama, H. *Chem.—Eur. J.* **2010**, 16, 3090. (k) Castro, L. C. M.; Bézier, D.; Sortais, J.-B.; Darcel, C. *Adv. Synth. Catal.* **2011**, 353, 1279. (l) Bhattacharya, P.; Krause, J. A.; Guan, H. *Organometallics* **2011**, 30, 4720. (m) Buitrago, E.; Zani, L.; Adolfsson, H. *Appl. Organomet. Chem.* **2011**, 25, 748. (n) Dieskau, A. P.; Begouin, J.-M.; Plietker, B. *Eur. J. Org. Chem.* **2011**, 5291. (o) Flückiger, M.; Togni, A. *Eur. J. Org. Chem.* **2011**, 4353. (p) Jiang, F.; Bézier, D.; Sortais, J.-B.; Darcel, C. *Adv. Synth. Catal.* **2011**, 353, 239. (q) Yu, S.; Shen, W.; Li, Y.; Dong, Z.; Xu, Y.; Li, Q.; Zhang, J.; Gao, J. *Adv. Synth. Catal.* **2012**, 354, 818. (r) Buitrago, E.; Tinnis, F.; Adolfsson, H. *Adv. Synth. Catal.* **2012**, 354, 217. (s) Bézier, D.; Jiang, F.; Roisnel, T.; Sortais, J.-B.; Darcel, C. *Eur. J. Inorg. Chem.* **2012**, 1333. (t) Hashimoto, T.; Urban, S.; Hoshino, R.; Ohki, Y.; Tatsumi, K.; Glorius, F. *Organometallics* **2012**, 31, 4474.
- (16) (a) Yang, J.; Tilley, T. D. *Angew. Chem., Int. Ed.* **2010**, 49, 10186. (b) Tondreau, A. M.; Lobkovsky, E.; Chirik, P. J. *Org. Lett.* **2008**, 10, 2789.
- (17) Bis(imino)pyridine iron complexes catalyze chemoselective hydrogenation of alkenes containing amide, ester, and ketone functionalities with hydrogen. See: (a) Russell, S. K.; Darmon, J. M.; Lobkovsky, E.; Chirik, P. J. *Inorg. Chem.* **2010**, 49, 2782. (b) Trovitch, R. J.; Lobkovsky, E.; Bill, E.; Chirik, P. J. *Organometallics* **2008**, 27, 1470. (c) Yu, R. P.; Darmon, J. M.; Hoyt, J. M.; Margulieux, G. W.; Turner, Z. R.; Chirik, P. J. *ACS Catalysis* **2012**, 2, 1760.
- (18) (a) Trovitch, R. J.; Lobkovsky, E.; Chirik, P. J. *Inorg. Chem.* **2006**, 45, 7252. (b) Zhang, J.; Gandelman, M.; Herrman, D.; Leituss, G.; Shimon, L. J. W.; Ben-David, Y.; Milstein, D. *Inorg. Chim. Acta* **2006**, 359, 1955. (c) Langer, R.; Leituss, G.; Ben-David, Y.; Milstein, D. *Angew. Chem., Int. Ed.* **2011**, 50, 2120. (d) Langer, R.; Iron, M. A.; Konstantinovskii, L.; Diskin-Posner, Y.; Leituss, G.; Ben-David, Y.; Milstein, D. *Chem.—Eur. J.* **2012**, 18, 7196. (e) Pelczar, E. M.; Emge, T. J.; Krogh-Jespersen, K.; Goldman, A. S. *Organometallics* **2008**, 27, 5759.
- (19) (a) Zhang, L.; Peng, D.; Leng, X.; Huang, Z. *Angew. Chem., Int. Ed.* **2013**, 52, 3676. Very recently, Chirik et al. reported (PDI)Fe-catalyzed alkene hydroboration. See: (b) Obligacion, J. V.; Chirik, P. J. *Org. Lett.* **2013**, 15, 2680.
- (20) This activation strategy was first reported by Chirik et al. for the in situ activation of (PDI)FeCl₂. See: Bouwkamp, M. W.; Bowman, A. C.; Lobkovsky, E.; Chirik, P. J. *J. Am. Chem. Soc.* **2006**, 128, 13340.
- (21) Control experiments with (i) the precatalyst **5a** and no NaBHET₃; and (ii) NaBHET₃, but with no **5a**, gave no alkene hydrosilylation product.
- (22) It should be noted that in all of the reactions involving (EtO)₃SiH, trace amounts of (EtO)₄Si (<5%) were detected by GC/MS resulting from redistribution of (EtO)₃SiH. Therefore, these reactions need to be carried out with care.
- (23) Tondreau, A. M.; Milsman, C.; Lobkovsky, E.; Chirik, P. J. *Inorg. Chem.* **2011**, 50, 9888.
- (24) Darmon, J. M.; Turner, Z. R.; Lobkovsky, E.; Chirik, P. J. *Organometallics* **2012**, 31, 2275.
- (25) Lu, C. C.; Weyhermüller, T.; Bill, E.; Wieghardt, K. *Inorg. Chem.* **2009**, 48, 6055.
- (26) Bart, S. C.; Chlopek, K.; Bill, E.; Bouwkamp, M. W.; Lobkovsky, E.; Neese, F.; Wieghardt, K.; Chirik, P. J. *J. Am. Chem. Soc.* **2006**, 128, 13901.
- (27) La Mar, G. N.; Horrocks, W. D.; Holm, R. H. *NMR of Paramagnetic Molecules*; Academic Press: New York, 1973; pp 85–178.
- (28) Liu, T.; Li, B.; Popescu, C. V.; Bilko, A.; Pérez, L. M.; Hall, M. B.; Darensbourg, M. Y. *Chem.—Eur. J.* **2010**, 16, 3083.
- (29) Wu, J. Y.; Stanzl, B. N.; Ritter, T. *J. Am. Chem. Soc.* **2010**, 132, 13214.
- (30) Because complex **5h** (^{IPr}PNN^H)FeBr₂ is the best precatalyst for chemoselective alkene hydrosilylation of **11**, the computations were performed on olefin- and O-bound (^{IPr}PNN^H) species.
- (31) Cook, C.; Guinchard, X.; Liron, F.; Roulland, E. *Org. Lett.* **2010**, 12, 744.
- (32) Mori, K. *Eur. J. Org. Chem.* **2005**, 2005, 2040.
- (33) Alcaide, B.; Almendros, P.; Alonso, J. M. *Chem.—Eur. J.* **2003**, 9, 5793.
- (34) Ginotra, S. K.; Friest, J. A.; Berkowitz, D. B. *Org. Lett.* **2012**, 14, 968.
- (35) Tauk, L.; Schroder, A. P.; Decher, G.; Giuseppone, N. *Nat. Chem.* **2009**, 1, 649.
- (36) Babler, J. H.; White, N. A.; Kowalski, E.; Jast, J. R. *Tetrahedron Lett.* **2011**, 52, 745.
- (37) Lanners, S.; Norouzi-Arasi, H.; Khiri, N.; Hanquet, G. *Eur. J. Org. Chem.* **2007**, 2007, 4065.
- (38) Schleicher, K. D.; Jamison, T. F. *Org. Lett.* **2007**, 9, 875.
- (39) Mpango, G. B.; Mahalanabis, K. K.; Mahdavi-Damghani, Z.; Snieckus, V. *Tetrahedron Lett.* **1980**, 21, 4823.
- (40) Rangheard, C.; H. Olivier-Bourbigou, Proriol, D.; , Inst. Français Du Pétrole, U.S. Pat. Appl. 2011009635, A1, 2011.
- (41) Chan, D. M. T.; Monaco, K. L.; Wang, R.-P.; Winters, M. P. *Tetrahedron Lett.* **1998**, 39, 2933.
- (42) Fujita, M.; Hiyama, T. *J. Org. Chem.* **1988**, 53, 5405.
- (43) Prediger, P.; Barbosa, L. F.; Génisson, Y.; Correia, C. R. D. *J. Org. Chem.* **2011**, 76, 7737.
- (44) Dash, A. K.; Gourevich, I.; Wang, J. Q.; Wang, J.; Kapon, M.; Eisen, M. S. *Organometallics* **2001**, 20, 5084.
- (45) Inubushi, H.; Kondo, H.; Lesbani, A.; Miyachi, M.; Yamanoi, Y.; Nishihara, H. *Chem. Commun.* **2013**, 134.
- (46) Frisch, M. J.; et al. *Gaussian 09*, Revision A.1; Gaussian, Inc.: Wallingford CT, 2009.